

1

## 2 **Environmentally-mediated selection parallels population 3 divergence across a chimpanzee subspecies contact zone**

4

5 Matthew W. Mitchell<sup>1,2,\*</sup>, Walker Alexander<sup>3</sup>, Dana V. Mitchell<sup>1</sup>, Adam H. Freedman<sup>4</sup>,  
6 Janina Dordel<sup>1</sup>, Ryan J. Harrigan<sup>5</sup>, Ahmet Sacan<sup>3</sup>, Fabrice Kentatchime<sup>1,6</sup>, Bryan S.  
7 Featherstone<sup>1</sup>, Ekwoge E. Abwe<sup>1,7,8</sup>, Paul R. Sesink Clee<sup>1</sup>, Abwe E. Abwe<sup>8</sup>, Sabrina  
8 Locatelli<sup>9</sup>, Bethan J. Morgan<sup>7,8,10</sup>, Bernard Fosso<sup>11</sup>, Roger Fotso<sup>11</sup>, Sarah A. Tishkoff<sup>12</sup>,  
9 Evan E. Eichler<sup>13,14</sup>, Nicola M. Anthony<sup>15</sup>, Thomas B. Smith<sup>5,16</sup>, Mary Katherine  
10 Gonder<sup>1,6,\*</sup>

11 <sup>1</sup>Department of Biology, Drexel University, Philadelphia, PA, USA

12 <sup>2</sup>Coriell Institute for Medical Research, Camden, NJ, USA

13 <sup>3</sup>School of Biomedical Engineering, Science and Health Systems, Drexel University,  
14 Philadelphia, PA, USA

15 <sup>4</sup>Faculty of Arts and Sciences Informatics Group, Harvard University, Cambridge, MA,  
16 USA

17 <sup>5</sup>Center for Tropical Research, Institute of Environment and Sustainability, University of  
18 California, Los Angeles, CA, USA

19 <sup>6</sup>Department of Ecology and Conservation Biology, Texas A&M University, College  
20 Station, TX, USA

21 <sup>7</sup>San Diego Zoo Wildlife Alliance, Escondido, CA, USA

22 <sup>8</sup>Cameroon Biodiversity Association, Douala, Cameroon

23 <sup>9</sup>Institut de Recherche pour le Développement (IRD), Maladies Infectieuses et Vecteurs:  
24 Ecologie, Génétique, Evolution et Contrôle (MIVEGEC) (IRD 224-CNRS 5290-  
25 Université de Montpellier), Montpellier, France

26 <sup>10</sup>School of Natural Sciences, University of Stirling, Stirling, UK

27 <sup>11</sup>Wildlife Conservation Society Cameroon, Yaoundé, Cameroon

28 <sup>12</sup>Departments of Genetics and Biology, University of Pennsylvania, Philadelphia, PA,  
29 USA

30 <sup>13</sup>Department of Genome Sciences, University of Washington School of Medicine,  
31 Seattle, WA, USA

32 <sup>14</sup>Howard Hughes Medical Institute, University of Washington, Seattle, WA, USA

33 <sup>15</sup>Department of Biological Sciences, University of New Orleans, New Orleans, LA, USA

34 <sup>16</sup>Department of Ecology and Evolutionary Biology, University of California, Los  
35 Angeles, CA, USA

36

37 \*Matthew W. Mitchell  
38 Email: mmitchell@coriell.org

39  
40 \*Mary Katherine Gonder  
41 katy.gonder@ag.tamu.edu

42

## 43 Abstract

44 Species evolve from populations with ancestor-descendant relationships in a bifurcating  
45 process shaped by geography, gene flow, genetic drift, and natural selection leading to  
46 local adaptation to prevailing environmental and ecological conditions. Building on this  
47 foundational understanding, we explored local adaptation in chimpanzees (*Pan*  
48 *troglodytes*) at a key geographical intersection in Cameroon where the two main  
49 chimpanzee phylogenetic lineages converge. The Nigeria-Cameroon chimpanzee (*P. t.*  
50 *ellioti*) and central chimpanzee (*P. t. troglodytes*) last shared a common ancestor about  
51 500 thousand years ago, with occasional gene flow between them. The evolutionary  
52 processes driving their prolonged separation are not fully understood, but neutral  
53 evolutionary mechanisms alone cannot account for the observed divergence pattern.  
54 Cameroon is often referred to as 'Africa in miniature' because the Gulf of Guinea Forest,  
55 Congo Basin Forest, and savanna converge there, forming an ecotone. Thus, this  
56 contact zone between subspecies in Cameroon provides a unique natural laboratory  
57 that enabled us to investigate how environmental variation and natural selection shape  
58 divergence in chimpanzees. We developed a genome-wide panel of single-nucleotide  
59 polymorphisms (SNPs) in 112 wild chimpanzees sampled in multiple habitats across  
60 this contact zone. We augmented SNP discovery by sequencing eight new chimpanzee  
61 genomes from Cameroon and analyzing them with previously published chimpanzee  
62 genomes. We found that *P. t. ellioti* and *P. t. troglodytes* diverged from one another  
63 around 478,000 years ago and occasionally exchange migrants. We identified 1,690  
64 unique SNPs across 905 genes associated with 31 environmental variables that  
65 describe the habitat. These genes are involved in essential biological processes,

66 including immune response, neurological development, behavior, and dietary  
67 adaptations. This study highlights the importance of understanding the geographical  
68 context of natural selection, paving the way for future studies to interpret evidence for  
69 genetic variation with phenotypic traits and deepening our understanding of how  
70 populations diverge in response to environmental pressures.

71

## 72 **Author Summary**

73 We investigated how local adaptation contributes to shaping the diversification of  
74 chimpanzee subspecies at the geographical convergence point for the two major  
75 branches of the chimpanzee phylogenetic tree. We analyzed genome-wide SNP  
76 genotypes of 112 chimpanzees sampled from natural communities located in this  
77 understudied area. We used tiered methods that identified 905 genes subject to  
78 selection, each associated with one or more of 31 environmental predictors describing  
79 the habitat. We found strong signals of selection in immune response genes that  
80 separate *P. t. troglodytes* from *P. t. elliotti*, highlighting the important role of different  
81 pathogen histories in their evolution. We also found evidence of selection in genes  
82 associated with neurological development, behavior, and diet, that separate both the  
83 subspecies and populations of *P. t. elliotti* that occupy different niches. These findings  
84 suggest that ecological and cultural factors may also contribute to shaping the  
85 diversification of chimpanzees across the contact zone.

86

## 87 **Introduction**

88       Species consist of populations of reproductively compatible individuals with  
89       ancestor–descendant relationships that evolve through time [1]. Speciation may result  
90       from various factors. It may have a geographical dimension ranging from allopatry to  
91       sympatry with varying degrees of gene flow among populations, genetic drift, and  
92       natural selection [2]. Ecological factors often play a decisive role in this process through  
93       the local adaptation of populations to prevailing environmental conditions [3]. The fusion  
94       of genomics with ecological modeling has advanced the ability to identify loci under  
95       environmental selection. It contributes to understanding how species adapt to specific  
96       habitats and its impact on speciation [4, 5]. While this link has been studied in many  
97       taxa [6], it has been an especially strong focus in studies of human evolution. Human  
98       populations have adapted to a multitude of environments [5], disease landscapes [4, 7,  
99       8], and diets including the ability to digest milk into adulthood [9], fatty acid digestion  
100       [10], foraging practices in tropical African rainforests [11], cereal-rich diets [12], and  
101       persistence in high-altitude environments [13-15].

102       By comparison, the factors that contribute to shaping the evolution of non-human  
103       great ape species are poorly understood. Genomic tools have contributed substantially  
104       to resolving the evolutionary relationships and histories of great ape species,  
105       subspecies, and some populations [16-20]. However, these studies generally assumed  
106       that neutral evolutionary processes (i.e., genetic drift) largely explain the partitioning of  
107       genetic variation in great apes. In particular, population genetic structure has been  
108       presented as evidence for allopatric speciation in 'Pleistocene Refugia,' among gorillas  
109       [21], isolation across conspicuous geographic boundaries like rivers [21-23], and

110 separation on different islands [20]. However, a growing body of evidence supports the  
111 hypothesis that local adaptation due to natural selection occupies an essential role in  
112 shaping the patterning of genetic variation and speciation in great apes [19, 24-26].

113 Among the great apes, chimpanzees (*Pan troglodytes*) have been particularly  
114 well-studied, including analysis of genomes from a representative sample of captive  
115 individuals [16, 18, 19] and population genetic studies of natural populations [22-24, 27].

116 The overall picture from these studies is that the species originated in western  
117 equatorial Africa about 1mya. By 500kya in the Middle Pleistocene, two lineages began  
118 to diverge from the ancestral *Pan* population: a western lineage composed of the  
119 subspecies *P. t. verus* and *P. t. elliotti*, and a central/eastern lineage comprising *P. t.*  
120 *troglodytes* and *P. t. schweinfurthii* (**Fig. 1a**). Major rivers, lakes, and the Dahomey Gap  
121 are thought to have acted as dispersal barriers that separate the subspecies to different  
122 degrees and timescales, potentially leading to allopatric speciation among chimpanzee  
123 subspecies. Among these dispersal barriers, the Sanaga River in Cameroon stands out  
124 (**Fig. 1b**). It separates the chimpanzee phylogenetic tree into its two main branches yet  
125 remains permeable to occasional gene flow between *P. t. elliotti* and *P. t. troglodytes*  
126 [18, 24, 27]. The Sanaga River has likely enabled some degree of allopatric divergence  
127 due to genetic drift but the role that natural selection may have played in separating  
128 these chimpanzee subspecies remains unknown.

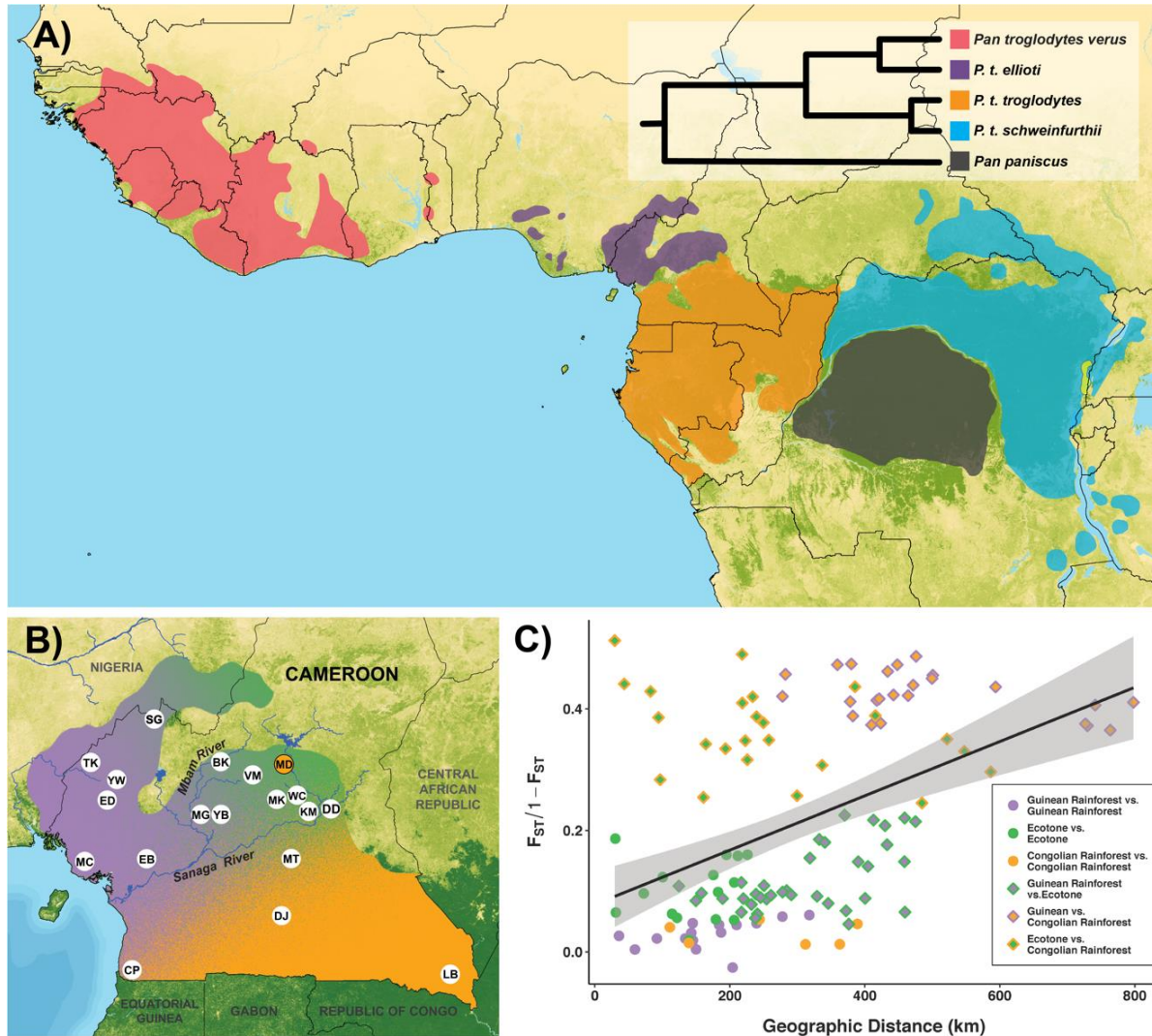


**Fig 1. Chimpanzee evolutionary history across Africa and population structure in Cameroon.**

(A) Distribution and phylogeny of the genus *Pan*.

(B) Sampling locations of wild chimpanzee populations in Cameroon overlaid on spatial interpolation of population structure using SNPs from wild chimpanzees. The 'MD' sampling location is shaded orange to signify the presence of a *P. t. ellioti*/*P. t. troglodytes* F1 hybrid (CMM06).

(C) Isolation-by-environment in wild chimpanzees in Cameroon. Correlation between 'linearized  $F_{ST}$ ' and geographic distance (km) generated using SNPs from wild chimpanzees. Solid circles represent pairs of sampling locations from the same habitat. Dual-colored diamonds represent pairs of sampling locations from different habitats. Colors correspond to chimpanzee population origin: purple – *P. t. ellioti* (Rainforest), green – *P. t. ellioti* (Ecotone), and orange – *P. t. troglodytes*.

129

130        Natural selection has numerous opportunities to contribute to genetic divergence

131        that may vary between subspecies or populations in different habitats. Life history traits

132 and pathogen defense stand out as likely candidates for establishing among-population  
133 divergence due to local adaptation. Among these, the role of pathogens is best  
134 understood. Differences in pathogen presence and prevalence have long been  
135 associated with genotypic differences among great apes, especially chimpanzees. For  
136 instance, wild chimpanzee populations are infected to different degrees with several  
137 disease-causing pathogens, including malaria [28], Ebola [29], and viruses like simian  
138 immunodeficiency virus (SIV) [30]. In the case of SIV and similar viruses, it is relatively  
139 well established that these pathogens have exerted selective pressure on chimpanzees,  
140 particularly the central and eastern subspecies [31-33]. Interestingly, Cameroon is a  
141 unique disease landscape for chimpanzees, especially concerning the puzzling  
142 distribution of SIVcpz. Unlike *P. t. troglodytes* and *P. t. schweinfurthii*, SIVcpz has not  
143 been found in *P. t. elliotti* or *P. t. verus*, despite extensive sampling [34-36] (**Fig. 1a**).

144 Secondly, each chimpanzee subspecies occupies a distinct set of environmental  
145 niches [37], creating opportunities for adaptation to local environmental conditions.  
146 Although little is known about the links among genotypes, phenotypes, and  
147 environmental conditions, chimpanzees in arid environments are more efficient in salt  
148 removal than their counterparts in more humid forested environments [38]. However,  
149 the role of local adaptation to specific environments remains largely unexplored yet is  
150 perhaps the most intriguing avenue of investigation in their evolution. Chimpanzees, like  
151 humans, have complex social systems and behaviors and maintain diverse cultural  
152 traditions [39]. Similarly, cultural variation among chimpanzee communities may lead to  
153 localized gene-culture co-evolution, potentially facilitating adaptation to diverse habitats  
154 [37] that are vulnerable to human encroachment [40]. Habitat variation and resource

155 availability, specifically food types, are also known to affect chimpanzee socioecological  
156 patterns directly [41], yet whether this variation translates into heritable genetic  
157 differences remains speculative.

158 We investigated how local adaptation has influenced the evolution of  
159 chimpanzees in Cameroon, a key region where the western and central/eastern  
160 lineages of chimpanzees converge. Despite the wealth of research on the contributions  
161 of neutral evolutionary processes to the genetic variation found in wild chimpanzees, the  
162 contribution of natural selection remains a significant knowledge gap that our study  
163 aimed to fill. We employed a two-tier approach to identify genic regions under selection  
164 from a comprehensive analysis of natural chimpanzee communities sampled intensively  
165 across Cameroon. First, we used whole-genome sequencing (WGS) data from 24  
166 previously published chimpanzee genomes [16], along with eight newly sequenced  
167 genomes of individuals from Cameroon to create and annotate a map of genomic  
168 regions under natural selection from this expanded sample of complete genomes of  
169 chimpanzees originating from Cameroon. Second, we used the analysis of this  
170 expanded sample of genomes to create a genome-wide panel of ancestry-informative  
171 putatively neutral SNPs, as well as SNPs that fell within signals of positive selection  
172 (inferred with the WGS data) and, thus, were good candidates for performing tests to  
173 assess local adaptation. We genotyped these SNPs in 112 wild chimpanzees sampled  
174 across multiple habitats in Cameroon, encircling the contact zone between *P. t. ellioti*  
175 and *P. t. troglodytes*, and that represent the diversity of habitats occupied by  
176 chimpanzees across the contact zone [42], including the northern extent of the Congo  
177 Basin Forest, the lowland and montane Gulf of Guinea Forest, and the forest/savanna

178 ecotone that bridges these two forest ecosystems. Finally, we used these SNP panels  
179 to investigate the relationship between individual SNPs and a suite of SNPs  
180 representing the genome to understand the relationship between allele frequencies and  
181 environmental variability. Our objective was to assess whether environmental pressures  
182 from differing ecologies have influenced allele frequency variation across these wild  
183 populations.

184

## 185 **Results**

186 We used WGS data from 24 previously published chimpanzee genomes [16],  
187 along with eight newly sequenced genomes of individuals from Cameroon from the  
188 Limbe Wildlife Center referred to hereafter as 'captive chimpanzees' (**Fig. S1** and **Table**  
189 **S1**). We used the captive chimpanzee dataset and previously published data [16] to  
190 create an annotated map of genomic regions under natural selection. Second, we used  
191 a genome-wide panel of SNPs in 112 wild chimpanzees sampled across multiple  
192 habitats across Cameroon (**Fig. 1b**) to develop a high-resolution, spatially explicit map  
193 of allele frequencies to understand the link between habitat variation and loci under  
194 selection.

## 195 **Captive chimpanzee genome analysis and SNP discovery**

### 196 **Developing SNP datasets**

197 We identified SNPs from 32 chimpanzee genomes across all four subspecies,  
198 which included eight newly sequenced genomes from the contact zone between the  
199 western and central/eastern chimpanzee lineages. After quality filtering, we retained

200 12,754,225 high-quality SNPs. Based on this initial whole-genome SNP set, two  
201 datasets were created. The first dataset was thinned for linkage disequilibrium (LD),  
202 retaining only SNPs with  $r^2 \leq 0.1$ , which resulted in 1,113,142 SNPs retained. The  
203 second dataset was thinned to include only SNPs that followed our neutrality criteria  
204 (**Methods**), resulting in 147,700 SNPs. **S1 Text** provides additional details on  
205 heterozygosity (**Fig. S2**) and population cluster analyses (**Figs. S3 and S4**).

206 **Genome scans for signals of selection and defining genomic ‘outlier’**  
207 **regions**

208 To calculate a test statistic for cross-population extended haplotype  
209 homozygosity (XP-EHH) and integrated haplotype score (iHS), SNP-based results were  
210 summarized into windows following Pickrell et al. [43], but chromosomes were split into  
211 100kb windows and SNPs were binned in 100 SNP increments. We merged windows  
212 indicating positive selection for each method and population. The analysis identified  
213 regions specific to the two lineages, and those shared among the Western and  
214 Central/Eastern lineages were analyzed separately. **Table 1** summarizes outlier regions  
215 for the XP-EHH and iHS and combined outlier tests. In the Western lineage, we found  
216 335 outlier windows stretching 83.5 Mb with 695 candidate genes. The Central/Eastern  
217 lineage had 318 windows stretching 81 Mb with 682 genes. We found 25 windows over  
218 13.6 Mb with 80 candidate genes shared between lineages. We plotted the distribution  
219 of the outlier regions on individual chromosomes (**Fig. 2a**).  
220

221 **Table 1. Summary of captive chimpanzee whole genome “outlier” regions.**

222

	XP-EHH		iHS		Combined		
	Western lineage	Central/ Eastern lineage	Western lineage	Central/ Eastern lineage	Western lineage	Central/ Eastern lineage	Shared
Windows found	257	270	118	95	335	318	25
Base pairs in windows	53,753,675	55,149,110	34,000,000	32,200,000	83,453,675	81,049,110	13,600,085
Protein coding genes used in enrichment analysis	563	563	152	144	695/610	682/593	80/70

223  
224

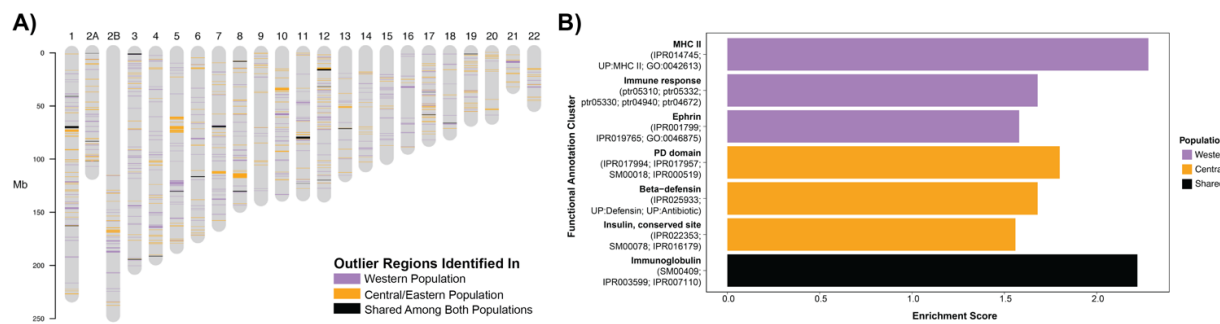


**Fig 2. Natural selection in chimpanzees.**

(A) Regions under selection found using captive chimpanzee genomes plotted on individual chromosomes.

(B) Functional enrichment clustering of genes and pathways under selection in chimpanzees. Enriched functional annotation clusters (based on genes in outlier regions) including their respective enrichment score. The name of one functional annotation of each cluster was taken to represent the complete cluster.

225

226

227 While all chromosomes are affected by selective sweeps some chromosomes  
228 show more regions under selection in one lineage or the other. The most extreme  
229 example in chimpanzees is chromosome 20, showing 6 times as many genetic regions  
230 under selection in the Central/Eastern lineage than in the Western lineage. Less  
231 extreme examples are found on chromosomes 8, 9, 13, and 19 with 2-fold more  
232 genome space showing evidence of selective sweeps in the Central/Eastern than the

233 Western lineage. In the Western lineage chromosomes 16, 15, 18, 3, and 11 show 5-,  
234 4-, 3-, 2-, and 2-fold more genome space to be under selection than the Central/Eastern  
235 lineage, respectively.

236 While the number of regions under selection in the Western as well as the  
237 Central/Eastern lineage was equal on chromosomes 1, 2A, 2B, 4-8, 10-14, and 17,  
238 there were some differences in the remaining chromosomes. Chromosomes 20 and 21  
239 in the Central/Eastern lineage had five and four times more regions affected by  
240 selective sweeps than the Western lineage. Chromosomes 9, 19, and 22 showed two  
241 times more regions. In the Western lineage chromosomes 16 and 15 exhibited four and  
242 three times more regions under selection than chromosomes in the Central/Eastern  
243 lineage. Chromosomes 3 and 18 showed two times more regions under selection in the  
244 Western lineage compared to the Central/Eastern lineage. There was no evidence for  
245 selection shared between both lineages on chromosomes 2B, 9, 10, 14-16, and 20, 21-  
246 22.

247 **Functional annotation, enrichment, and cluster analysis of outlier  
248 regions under selection**

249 We analyzed annotated outlier regions with complete or partially overlapping  
250 genes and other genetic content (e.g., non-coding genes, pseudogenes). Both lineages  
251 had significantly more protein-coding and non-coding genes than randomly sampled  
252 genome regions (one sample t-test,  $p=0.0001$  &  $p=0.0001$ ) (**Table 2**). Additionally, the  
253 number of non-coding genes (ncRNA) was also significantly higher (one sample t-test,  
254  $p=0.0001$  &  $p=0.0016$ ), while the number of pseudogenes showed no significant  
255 differences (one sample t-test,  $p=0.3023$  &  $p=0.6518$ ) (**Table 2**). Closer inspection of

256 the most enriched regions (**Table S2**) revealed these contained mostly protein-coding  
257 genes and ncRNAs. The region with the highest significance value in the Western  
258 lineage carries exclusively ncRNAs and one window did not contain any annotated  
259 genetic features at all.

260

261 **Table 2. Genetic content of 200 kb windows under selection and ten randomly**  
262 **sampled genome regions.**

POPULATION	Real Regions	Random Regions (n=10)		p-value <sup>a</sup>
		Average	StDev <sup>b</sup>	
<b>WEST</b>				
Protein coding genes	500	400.8	31.84	0.0001
ncRNAs	178	141.1	18.60	0.0001
Pseudogenes	5	6.2	2.90	0.3023
<b>CENTRAL/EAST</b>				
Protein coding genes	536	401.1	30.65	0.0001
ncRNAs	155	136.7	24.00	0.0016
Pseudogenes	5	6.4	2.72	0.6518

264  
265 <sup>a</sup>p-values were obtained using the “one sample t-test”.  
266 <sup>b</sup>StDev: Standard Deviation

267  
268 We examined enriched gene ontology (GO) terms in the ‘Biological Processes’  
269 category (**Table S3**) and enriched KEGG pathways (**Table S4**) for genes under  
270 selection in the Western lineage, the Central/Eastern lineage, or shared between the  
271 two populations. Genes significantly enriched in the Western lineage are involved in  
272 developmental processes (hair follicle development, embryonic development, pattern  
273 specification, melanocyte differentiation), cellular and metabolic processes, and protein  
274 localization and degradation. Enriched KEGG pathways in the Western lineage were  
275 mainly related to diseases caused by pathogens or internal dysfunctions, branched-  
276 chain amino acids (BCAAs) degradation, and neurological development. The

277 Central/Eastern lineage genes are enriched for innate immune system response,  
278 cellular processes, and wound healing. Enriched KEGG pathways in the  
279 Central/Eastern lineage are involved in several diseases affecting the heart muscle and  
280 Amoebiasis. The shared dataset showed enrichment only in bone mineralization without  
281 any KEGG pathway.

282 To minimize annotation redundancy and clarify the biological functions in each  
283 lineage, we grouped genes into functional clusters based on similar biological meaning,  
284 not physical distance [44]. **Fig 2b** and **Table S5** show functional enrichment clusters of  
285 genes that were unique to the western group (purple), unique to the central/eastern  
286 group (orange) and shared between the western and central/eastern lineage.

287 We grouped 610 candidate genes from the Western lineage into three clusters.  
288 The cluster with the highest enrichment score (ES = 2.3) included four genes (PATR-  
289 DOB, PATR-DMB, MAMU-DMA, HLA-DOA) functionally associated with the Major  
290 Histocompatibility Complex (MHC) II (**Fig. 3a**). MHC II genes, located on chromosome  
291 6, play a crucial role in the adaptive immune response by activating CD4 T cells to  
292 respond to extracellular pathogens [45]. The second cluster (ES = 1.8) contains the  
293 same four genes as the first cluster, plus gene HLA-DQA1. This cluster is defined by  
294 additional gene functions and displays enrichment in additional disease pathways active  
295 in diseases like Asthma, Graft-versus-host disease, Allograft rejection, type I diabetes  
296 mellitus, and the intestinal immune network for IgA production [45]. The third cluster (ES  
297 1.58) contains three genes containing the Ephrin receptor-binding domain. These three  
298 genes (EFNA4, EFNA3, EFNA1) form a gene cluster on chromosome 1 from position  
299 133,320,040 to 133,391,332. Depending on the context, Eph signaling pathways are

300 key determinants of neurological development, cell morphogenesis, tissue patterning,  
301 angiogenesis, and neural plasticity [46, 47].

302

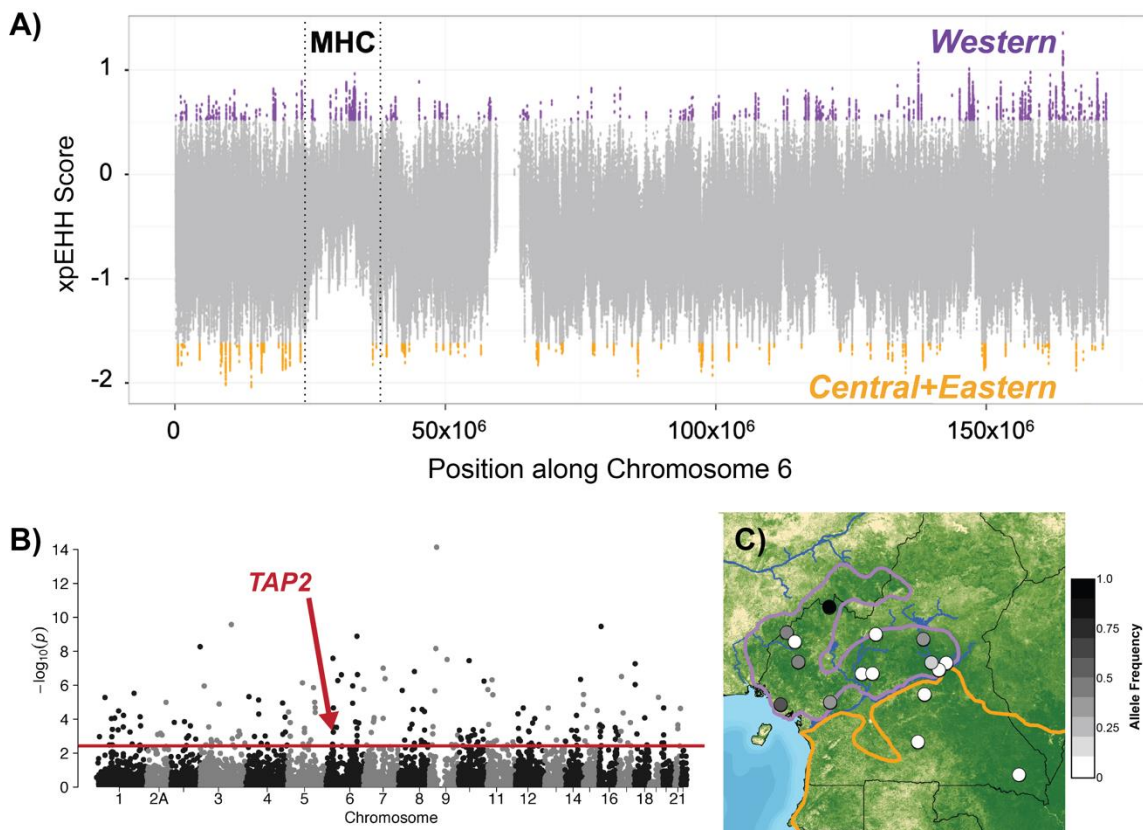


**Fig 3. Genome-wide variation of immune response genes under selection in chimpanzees.**

(A) XP-EHH analysis of SNPs on chromosome 6 from whole genome sequences of captive chimpanzees. Colored points represent SNPs within the 1% tail of the XP-EHH scores across the genome. The entire MHC region is noted, showing SNPs in MHC genes under selection in the Western lineage (*P. t. verus* and *P. t. ellioti*).

(B) Manhattan plot shows the genome-wide significance level (solid red line) for SNPs associated with Normalized Difference Vegetation Index (NDVI) - Brown with the *TAP2* SNP noted.

(C) Map of allele frequencies for the *TAP2* SNP superimposed onto NDVI and chimpanzee subspecies ranges in Cameroon.

303

304 In the Central/Eastern lineage, 593 genes were analyzed, forming three  
305 functional clusters. The first (ES=1.8) showed enrichment of three genes (TFF3, TFF2,  
306 TFF1) with a PD (or trefoil) domain. These three genes form a cluster on chromosome  
307 21, but their functions are not understood: The peptides coded for in these segments

308 are in several tissues but are most abundant in the GI tract where they may stabilize the  
309 mucosa and promote healing [48]. The second cluster (ES=1.7) contained five genes  
310 belonging to the beta-defensin gene including DEFB126, DEFB127, DEFB129, and  
311 DEFB132 are located on chromosome 20, and DEFB125 on chromosome 8. As  
312 antimicrobial peptides they are important in the innate response, including resistance of  
313 epithelial surfaces to microbial colonization and encapsulating viruses [49]. The third  
314 cluster (ES=1.6) comprises genes INS, RLN3, and INSL6, all sharing an Insulin-like  
315 domain.

316 Functional enrichment analysis of genes shared between both lineages revealed  
317 only one cluster of six genes with an enrichment score of 2.2: IL1RL2 and IL18RAP  
318 form a gene cluster on chr2A, CNTN6 is located on chr3, and ROBO3, ROBO4, and  
319 HEPACAM form a gene cluster on chr11. These genes are all annotated with an  
320 Immunoglobulin-like domain.

321 **Wild chimpanzee SNP genotyping, population structure, and**  
322 **selection analysis**

323 **Sequence analysis, filtering, SNP calling, and on-target read**  
324 **assessment**

325 We isolated DNA from fecal samples collected non-invasively from unhabituated  
326 natural communities of chimpanzees sampled across Cameroon. For 192 of these  
327 samples, we obtained 412,081,940 raw reads from single Illumina HiSeq PE125 lane –  
328 an average of ~2.15 million reads per sample. In total, 275,443,720 of these reads  
329 mapped to the chimpanzee reference genome; from these, we removed approximately

330 75 million reads and were left with 38,657,083 reads that mapped to our target sites  
331 (**Fig. S5a**) – an average of 201,339 on-target reads per sample. The 9,986 targeted  
332 sites had a mean read depth of 20x with one site showing as much as 166x coverage  
333 (**Fig. S6**). After removing samples for missing data and relatedness, we were left with  
334 two datasets ('10k' and '1k'). The '10k dataset' samples had significantly more on-target  
335 reads per sample than the total dataset; an average of 328,863 on-target reads per  
336 sample, representing ~16% of the total reads from these samples (**Figs. S5b and S5d**).  
337 The '10k dataset' filtering process resulted in 7,878 SNPs and 112 samples, and all  
338 samples from Boumba Bek (BB) and Campo Ma'an (CP) were removed. To retain more  
339 geographic representation of samples from at least one of these sites, we created  
340 another dataset ('1k dataset') by applying a more stringent site filter and the same  
341 individual missingness filter above which resulted in 994 SNPs and 142 samples  
342 (including two individuals from CP, but none from BB). The '1k dataset' samples had an  
343 average of 268,773 on-target reads per sample, representing ~12% of the total reads  
344 from these samples (**Figs. S5b and S5f**).

### 345 **Testing for isolation-by-distance and isolation-by-environment**

346 We found that pairwise  $F_{ST}$  values between sampling locations from different  
347 habitats were significantly higher than pairwise  $F_{ST}$  between sampling locations within  
348 the same habitat for both the '10k' (one-tailed  $t$ -test,  $p$ -value = 2.2e-16; **Figs. 1c** and  
349 **S7a**) and the '1k' dataset (one-tailed  $t$ -test,  $p$ -value = 2.1e-16; **Fig. S7b** and **S9a**).  
350 Additionally, the geographic distance between sampling locations from different habitats

351 was significantly higher than between locations within the same habitat for all 19  
352 sampling locations included in this study (one-tailed *t*-test, *p*-value = 6.324e-11).

353 We also performed a permutation test to account for the fact that population  
354 structure across habitats can confound the detection of isolation-by-distance (IBD). This  
355 categorized population pairs by geographic distance and randomized their habitat  
356 origins, forming a null distribution of *t*-statistics. Using this distribution, we assessed if  
357  $F_{ST}$  differed more between than within habitats/populations. For the '10k' and '1k'  
358 datasets, we found that  $F_{ST}$  was significantly higher between populations/habitats than  
359 within them (*p*-value < 0.0001; **Figs. S8b** and **S9b**). This suggests that IBD alone  
360 cannot fully explain the high  $F_{ST}$  values between populations/habitats. We also ran the  
361 permutation test for *P. t. ellioti* sampling locations alone and found that  $F_{ST}$  is  
362 significantly higher between *P. t. ellioti* (Rainforest) and *P. t. ellioti* (Ecotone) than within  
363 them compared to the null distribution (*p*-value = 0.0002; **Fig. S10**). Taken together, the  
364 results of the permutation tests suggest that habitat differences play a much stronger  
365 role than geographic distance alone, although the signal is slightly stronger within *P. t.*  
366 *ellioti* than in *P. t. troglodytes*. This may be attributed to the fact that *P. t. troglodytes* in  
367 Cameroon occupies more uniform Congo Basin forested habitat south and east of the  
368 Sanaga River. In contrast, *P. t. ellioti* occupies the comparatively diverse Gulf of Guinea  
369 forest comprising lowland forest, montane forest, and the forest-savanna gradient north  
370 of the Sanaga River.

371

## 372 Population structure, hybridization, and demographic history

373 We next investigated population structure, hybridization, and demographic  
374 history. Principal Components Analysis (PCA) (**Figs. S11, S12, S13, S14** and **Table**  
375 **S10**), population clustering analysis results (**Figs. S15** and **S16**), and Analysis of  
376 Molecular Variance (AMOVA) (**Table S11**) consistently distinguished between *P. t.*  
377 *elliotti* and *P. t. troglodytes*. The results from wild chimpanzee samples were consistent  
378 with results from the genome analysis of captive individuals (**Figs. S17, S18, S19, S20**  
379 and **S21**), indicating that our SNP discovery approach from captive individuals is likely  
380 capturing pockets of genetic differentiation present in wild individuals. In addition,  
381 certain individuals showed hybrid ancestry, notably an F1 hybrid in the *P. t. elliotti*  
382 population and a potential backcrossed hybrid in *P. t. troglodytes*. The demographic  
383 history model indicates that *P. t. elliotti* and *P. t. troglodytes* split from one another  
384 around 478,000 years ago, with continuous but rare gene flow between them since  
385 splitting, underlining a complex demographic history characterized by significant  
386 admixture and evolutionary divergence within the region. **S1 Text** provides more  
387 detailed results from these analyses. Based on these results, we concluded that neither  
388 the IBD model nor simple allopatric divergence along the banks of the Sanaga River  
389 fully explains the separation of *P. t. elliotti* from *P. t. troglodytes*.

## 390 Mapping wild chimpanzee genomic variation across habitats

391 These findings drew our attention to investigating how habitat variation  
392 corresponds with neutral and adaptive genetic differentiation among chimpanzees in  
393 Cameroon. Using a gradient forest model [50] and 31 environmental predictor variables

394 sourced from publicly available databases (See **Methods**, **SI Text**, and **Table S7**), we  
395 quantified environmental associations with genomic loci, pinpointing key environmental  
396 drivers and projecting genomic diversity spatially. We identified 581 SNPs with  
397 significant environmental associations, representing 6% of all SNPs from wild  
398 chimpanzees genotyped in this study. From these, 346 unique candidate genes within  
399 10kb windows of these SNPs, matched outliers from captive chimpanzee genome  
400 scans. When mapped to the study, these showed clear signals driven by a phylogenetic  
401 split between *P. t. ellioti* and *P. t. troglodytes* across the Sanaga River and habitat  
402 variation across Cameroon (**Fig. 4c**). Latitude (a proxy for geographic distance) had a  
403 pronounced effect along PC1 (**Fig. 4d**). Isothermality and surface moisture also  
404 contributed heavily to the model in differentiating between coastal and interior rainforest  
405 habitats, as well as rainforest versus ecotone habitats (**Fig. 4c** and **4d**).

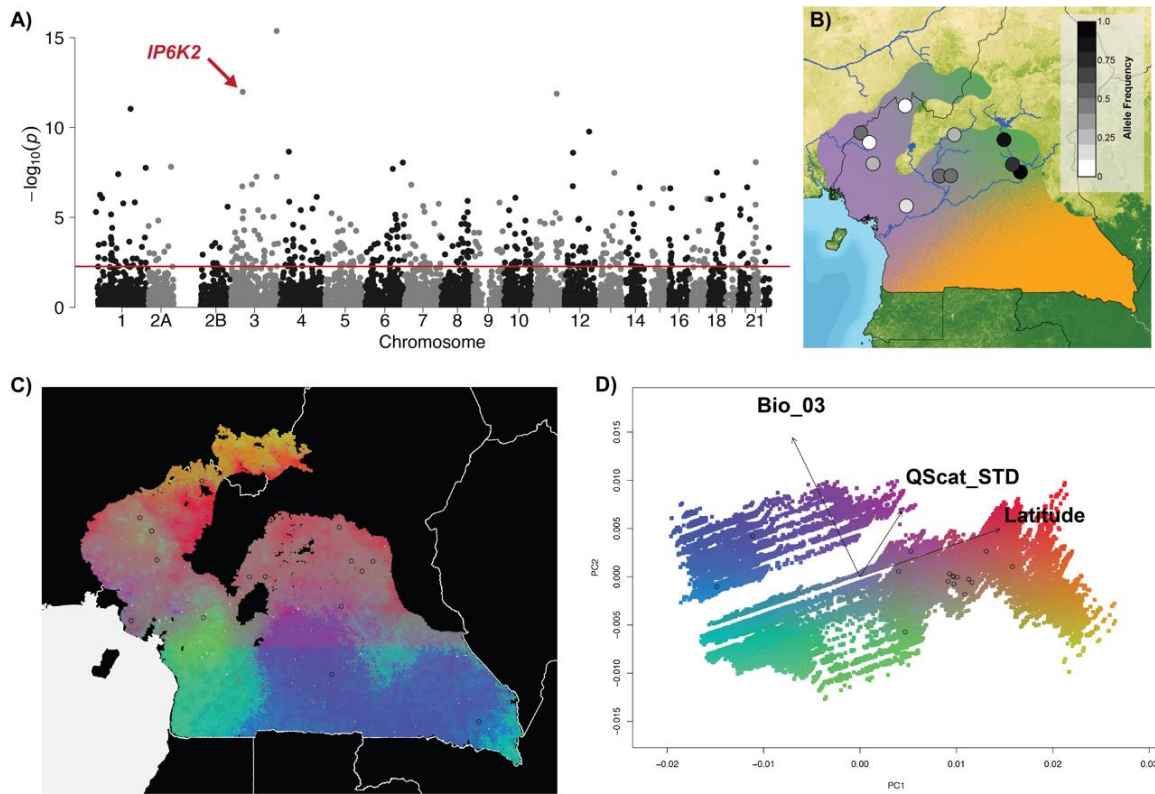


**Fig 4. Dietary gene under selection and gene-environment relationships.**

(A) Manhattan plot shows the genome-wide significance level (solid red line) for SNPs associated with Annual Mean Temperature (BIO1) with the *IP6K2* SNP noted.

(B) Spatialized allele frequencies for the *IP6K2* SNP showing differentiation between *P. t. ellioti* populations.

(C) Gradient forest-transformed climate variables show climate adaptation across the study area.

(D) Colors are based on a PCA of transformed climate variables.

406

407 Among all predictors tested in the model, latitude had the highest  $R^2$  weighted  
408 importance, likely reflecting the deep split between chimpanzee subspecies and/or  
409 bioclimate turnover across the rainforest-savanna gradient. Precipitation during the dry  
410 season and vegetation density were also important for predicting chimpanzee genomic  
411 diversity (Fig. S24). The second most important axis of variation in the gradient forest  
412 model primarily contributed to isothermality (bio3) and surface moisture (QScat\_STD).  
413 Thus, the variables contributing the most align with a rainforest/savanna ecotone split

414 (Figs. 4c and 4d), consistent with previous studies of niche modeling [42].

415 **Detecting environmentally associated loci under selection in wild**  
416 **chimpanzee populations**

417 We used Latent Factor Mixed Models (LFMM) to test for signals of selection on  
418 individual SNPs in a manner that controls for confounding effects of population  
419 structure. We identified 1,690 SNPs significantly associated with one of 31  
420 environmental predictors (**Table S7**) after accounting for population structure (K=3). We  
421 then identified 905 unique candidate genes within 10kb windows of the environmentally  
422 associated outlier SNPs, all of which were outliers in the captive chimpanzee genomes  
423 selection scan. Of the population groupings, we identified 695 associated with General  
424 Temperature variables, 388 associated with Temperature Range, 66 associated with  
425 Temperature Seasonality, 160 associated with Precipitation (Wet/Cold), 305 associated  
426 with Precipitation (Dry/Warm), 456 associated with Surface Moisture, 448 associated  
427 with Tree Cover, 355 associated with Vegetation Greenness, 325 associated with  
428 Vegetation Brownness, and 428 associated with Topography. A simple Mantel test  
429 revealed a significant correlation between pairs of environmental predictor variables and  
430 shared outlier SNPs returned by LFMM between variable pairs (Mantel  $r = 0.425$ ,  $p =$   
431  $1.00\text{e-}6$ ) demonstrating that independent LFMM performed as expected.

432 **Quantifying environmental relationships with candidate genes**

433 We searched for functional enrichment signals in environment-associated genes  
434 in two complementary ways. First, we compared the functions of genes associated with  
435 environmental variation with genes that show no signs of positive selection. This  
436 comparison helped us determine whether genes influenced by environmental factors

437 and potentially under selection differ functionally from those evolving under neutral  
438 conditions. We used genes outside outlier regions from the captive chimpanzee whole-  
439 genome analysis as a reference. We identified 47 biological processes enriched in  
440 1,018 unique environmentally associated outlier genes from both the gradient forest and  
441 LFMM models (**Table S12**). There were several enrichment clusters, notably two  
442 processes functionally associated with immune response, one was related to the Major  
443 Histocompatibility Complex (MHC) II – an important part of the adaptive immune system  
444 - and eight processes associated with neurological development, including 60 unique  
445 genes. We also found 48 enriched KEGG pathways in this subset of outliers (**Table**  
446 **S13**). Key clusters included pathways in neurological development (56 genes), digestion  
447 and metabolism (40 genes), and immune response (40 genes).

448 Our second analysis examined if genes influenced by environmental variation  
449 showed functional enrichments compared to those under positive selection without a  
450 clear environmental impact. This test uses a much smaller set of background genes  
451 composed only of those assayed in wild chimpanzee SNP scan but were not  
452 environmentally associated outliers in the LFMM and gradient forest models.  
453 Unsurprisingly, the enrichment analysis using this more limited background set of genes  
454 resulted in one significantly enriched biological process and KEGG pathway each, both  
455 relating to neurological development, specifically axon guidance (**Table S14**).

456 Of the genes linked with immune response and MHC II, Transporter 2, ATP  
457 binding cassette subfamily B member (*TAP2*) stands out. It contains a SNP that  
458 significantly associated with Vegetation Brownness (NDVI BRN) ( $-\log_{10} = 3.231762344$ ,  
459  $p < 0.001$ ) (**Fig. 3b**) and is associated with *General Temperature* variables in the LFMM

460 analysis of wild chimpanzees. The *TAP2* SNP in wild chimpanzees is nearly fixed in *P.*  
461 *t. troglodytes* and is variable across *P. t. ellioti* habitats (**Fig. 3c**). Additionally, *TAP2* was  
462 found to be under natural selection in the analysis of captive chimpanzee whole  
463 genomes, and it is part of the enriched KEGG pathways under selection in *P. t. verus*  
464 and *P. t. ellioti* (**Table S4**). *TAP2* is a component of the transporter associated with  
465 antigen processing (TAP) complex, which plays a role in ensuring that MHC class I  
466 (MHC-I) molecules are expressed on the cell surface [51]. TAP complex proteins,  
467 including *TAP2*, are essential for viral peptide transport from the cytoplasm onto MHC-I  
468 receptors within the endoplasmic reticulum [52]. In humans, several *TAP2* gene variants  
469 are linked to an increased HIV-1 infection risk [53].

470 We identified the gene, Leucine rich repeat and Ig domain containing 2  
471 (*LINGO2*), as having one of the strongest associations with the environmental predictor  
472 variable, mean annual normalized vegetation index (NDVI), in the LFMM analysis ( $-\log_{10}$   
473  $= 8.32330639$ ,  $p = 0.0000000475$ ) (**Fig. 5a**). A linear regression also revealed a  
474 significant association between the allele frequencies of the *LINGO2* SNP and mean  
475 annual NDVI ( $R^2 = 0.4826$ ,  $p = 0.003495$ ) (**Fig. 5b**). Low allele frequencies were found  
476 in *P. t. ellioti* (Rainforest), with variable frequencies found in *P. t. ellioti* (Ecotone) (**Fig.**  
477 **5c**). *LINGO2* is highly expressed in human brain tissue [54] and affects synapse  
478 development and function [55]. *LINGO2* is also under positive selection in Lidia cattle  
479 breed subpopulations and partially drives neurobehavioral phenotype variation among  
480 them [56].

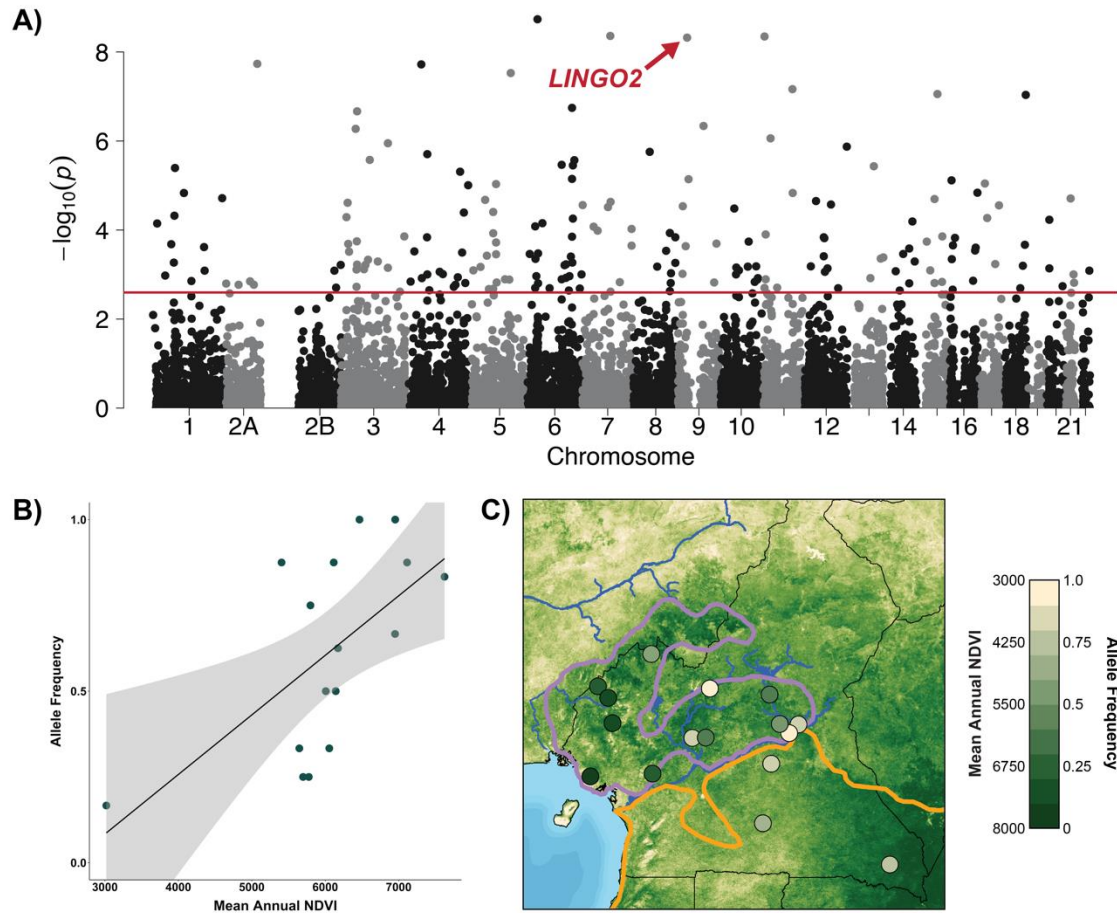


**Fig 5. Genome-wide variation of neurological development genes under selection.**

(A) Manhattan plot shows the genome-wide significance level (solid red line) for SNPs association with mean annual normalized vegetation index (NDVI) with the *LINGO2* SNP noted.

(B) Correlation between *LINGO2* allele frequency and mean annual NDVI.

(C) Spatialization of allele frequencies for this SNP superimposed onto mean annual NDVI.

481

482        Of the 24 digestion and metabolism-related genes identified in the biological  
483        processes and KEGG pathways, we further narrowed down our search by using  
484        additional measures to quantify relationships of each of the genes with environmental  
485        variables and were able to identify two genes with associated SNPs exhibiting  
486        significant linear relationships directly with their associated environmental variables  
487        across space, suggesting a potential role for diversifying selection across the  
488        forest/savanna ecotone gradient. Acetyl-CoA acetyltransferase 2 (ACAT2) contains the

489 SNP at position 161,530,902 on chromosome 6 (**Fig. S26a**), which had the strongest  
490 association of all SNPs with temperature seasonality according to results of the LFMM  
491 analysis ( $-\log_{10} = 3.594887672$ ,  $p = 0.000254163$ ) (**Fig. S26b**). Linear regression  
492 revealed a strong and significant relationship between *ACAT2*'s outlier SNP and  
493 temperature seasonality ( $R^2 = 0.5651$ ,  $p = 0.0005$ ) (**Fig. S26c**). When plotting allele  
494 frequencies of *ACAT2*'s outlier SNP, higher frequencies were observed in the ecotone's  
495 northern sampling sites. Sampling sites within the range of the *P. t. troglodytes*  
496 population had lower frequencies of the allele (**Fig. S26d**). The product of the *ACAT2*  
497 gene is known to be involved in cholesterol and beta-oxidation lipid metabolism [57].

498 Another gene identified to have an environmentally associated outlier SNP was  
499 Phospholipase C like 2 (*PLCL2*). *PLCL2* contains the SNP at position 17,268,745 on  
500 chromosome 3 (**Fig. S27a**). We identified a strong relationship between this SNP and  
501 the environmental variable *precipitation of the wettest month* through LFMM analysis ( $-\log_{10} = 3.36472742$ ,  $p = 0.00043179$ ) (**Fig. S27b**). Linear regression revealed a strong  
502 and significant relationship between *PLCL2*'s outlier SNP and the environmental  
503 variable *precipitation of the wettest month* ( $R^2 = 0.3422$ ,  $p = 0.0102$ ) (**Fig. S27c**). We  
504 observed higher allele frequencies of the *PLCL2* SNP in the *P. t. ellioti* ecotone  
505 population, with the *P. t. ellioti* rainforest population having the lowest frequencies  
506 across Cameroon (**Fig. S27d**). *PLCL2* is associated with obesity in mouse models.  
507 Individuals lacking the allele were shown to have a leaner phenotype; were able to  
508 resist induced obesity due to increased protection from glucose metabolism disorders  
509 and insulin resistance; and exhibited higher energy expenditure [58].

511 Finally, a SNP in the Inositol hexakisphosphate kinase 2 (*IP6K2*) gene was

512 identified as a significant outlier differentiating the *P. t. ellioti* ecotone and rainforest  
513 populations and associated with the environmental variable *Mean Annual Temperature*  
514 through LFMM analysis ( $-\log_{10} = 11.98296666$ ,  $p < 0.0001$ ) (**Fig. 4a**). *IP6K2*'s SNP was  
515 significantly more divergent than neutral SNPs between the two *P. t. ellioti* populations  
516 ( $F_{ST} = 0.49$ ,  $p < 0.0001$ ) (**Fig. 4b**). In humans, the *IP6K2* gene is linked with  
517 inflammatory bowel disease and cellular response to flavonoids, plant metabolites found  
518 in fruits and vegetables [59]. The human KEGG pathway containing *IP6K2* is associated  
519 with VACTERL/VATER syndrome, often associated with congenital heart disease and  
520 chondrodysplasia [60, 61].

521

## 522 Discussion

523 We presented genome-wide SNP genotyping from a representative sample of  
524 112 wild chimpanzees from across Cameroon, along with eight newly sequenced  
525 genomes of captive chimpanzees to enhance SNP discovery. We supplemented these  
526 data by combining genetic analyses with environmental association scans to search for  
527 evidence of environmentally-mediated selection. While prior studies have largely  
528 concentrated on neutral evolution mechanisms across this contact zone between  
529 chimpanzee lineages, our findings support a role for diversifying selection in the  
530 divergence of chimpanzee subspecies across different environments. The proposed  
531 population history of chimpanzees across this contact zone is well supported in this  
532 study. *P. t. ellioti* and *P. t. troglodytes* last shared a common ancestor around 478,000  
533 years ago, with occasional gene flow between them evidenced by an F1 hybrid in *P. t.*

534 *ellioti* and a potential backcrossed hybrid in *P. t. troglodytes*. These findings support  
535 prior studies suggesting that this contact zone between subspecies best fits an  
536 isolation-with-migration population model in which allopatric divergence and positive  
537 selection contribute to the partitioning of genetic variation [62].

538 The evidence supporting a role for environmentally-mediated selection across  
539 this contact zone is also compelling. We found 1,690 unique SNPs were associated with  
540 at least one of 31 environmental predictors, indicating that prevailing environmental  
541 conditions contribute to local adaptation in *P. t. ellioti* and *P. t. troglodytes*, and to a  
542 lesser extent, among populations within *P. t. ellioti*. These SNPs are distributed among  
543 905 outlier genes enriched for 48 biological processes. Overall, the sets of genes with  
544 highly divergent allele frequencies that separate *P. t. ellioti* from *P. t. troglodytes*  
545 suggest a role for selection in pathways important in two main categories: immune  
546 response and life history traits (neurological development, behavior, and dietary  
547 function).

548 It is important to reiterate that all outliers identified in wild chimpanzees using  
549 LFMM-based approaches were also identified as outliers in the haplotype homozygosity  
550 selection scans of captive chimpanzee genomes. This two-tiered approach offers  
551 heightened reliability of selection scans in wild populations while mitigating the  
552 incidence of false positives in our final dataset. Moreover, the congruence of these  
553 identified genomic regions between the two methods and two complementary datasets  
554 suggests that these outliers are subject to positive selection and not merely an artifact  
555 of demographic history or neutral population genetic structure.

556

## 557 **Signatures of selection from variable pathogen histories**

558        The lack of natural SIVcpz infection in *P. t. ellioti* sparks interest because it  
559    persists despite opportunities for transmission. SIVcpz*Ptt* virus infects *P. t. troglodytes*,  
560    crossed the species barrier on at least four occasions: from chimpanzees to humans in  
561    southern Cameroon, giving rise to the HIV-1 group M pandemic and to HIV-1 group N  
562    [63, 64]. HIV-1 group O and P also arose from transmission from chimpanzees to  
563    gorillas before subsequent transmission to humans [65, 66]. Thus, SIVcpz can cross  
564    genus boundaries which makes its absence in *P. t. ellioti* particularly striking since this  
565    subspecies still exchanges occasional migrants with *P. t. troglodytes*. Finally, the  
566    presence of prey primate species that harbor endemic SIV strains also creates multiple  
567    pathways for cross-species transmissions [34, 36, 67, 68]. Thus, we speculate that the  
568    absence of an SIVcpz in *P. t. ellioti* must be at least partially explained by adaptations  
569    that interrupt SIVcpz cell entry and/or boost immune response to clear SIVcpz infection.

570        Four processes functionally associated with the Major Histocompatibility  
571    Complex (MHC) II on chromosome 6 play a crucial role in the adaptive immune  
572    response. MHC II peptides stimulate CD4+ T cells that activate downstream immune  
573    responses to intracellular pathogens, including viruses. In particular, the Th1/Th2 cell  
574    differentiation pathway determines the type of helper cell a CD4+ T cell will become.  
575    Naïve CD4+ T cells recognize an MHC class II molecule, activate, and divide to produce  
576    clone effector CD4+ T cells specific for a particular antigen. CD4+ T cells can  
577    differentiate into T helper type-1 (Th1), T helper type-2 (Th2), or other T helper types,  
578    each with distinct cytokine-secretion phenotypes, production of distinct interferons, and  
579    different downstream immune responses. This finding corresponds well with a growing

580 body of evidence that positive selection associated with pathogen defenses has  
581 contributed to the genetic and phenotypic differentiation of chimpanzee subspecies,  
582 especially *P. t. troglodytes* and *P. t schweinfurthii*, which is perhaps due to exposure to  
583 different viruses [32].

584 This finding naturally called our attention to the absence of SIVcpz in *P. t. ellioti*  
585 attributed to a lack of gene flow between *P. t. ellioti* and *P. t. troglodytes* [30]. Given that  
586 gene flow occurs between *P. t. ellioti* and *P. t. troglodytes*, and that SIVcpzptt *P. t.*  
587 *troglodytes* is the source of multiple cross-species infections in both humans and  
588 gorillas, it is logical to assume that SIVcpz should naturally infect *P. t. ellioti*. We  
589 observed evidence of positive selection in *P. t. ellioti* due to highly differentiated SNPs  
590 enriched in genic sites. Among these, *TAP2* (**Fig. 3c**) variants increase the risk of HIV  
591 infection in humans [53], and may have a similar function in chimpanzees. Given the  
592 low level of gene flow, and the absence of sequence data upstream or downstream of  
593 the *TAP2* in our data, we cannot conclude whether this is evidence for recent adaptation  
594 to SIVcpzptt or evidence of ancient selection resulting from exposure to SIV-like viruses.  
595 Evidence is mounting that chimpanzees have had a long and continuing relationship  
596 with SIV-like viruses such that differences in viral exposures and immune responses  
597 have likely been a central feature of the evolution of chimpanzees [32, 33, 69].

598 For instance, *P. t. troglodytes* and *P. t. schweinfurthii* also show evidence of  
599 recent positive selection in genes involved in SIV/HIV cell entry and immune response  
600 to SIV, biological pathways responsible for T-helper cell differentiation, including CD4  
601 [33], and multiple genes that SIV/HIV use to infect and control host cells including  
602 CCR3, CCR9 and CXCR6 [32]. There is also compelling evidence of past selective

603 sweeps leading to reduced diversity in the MHC II repertoire of *P. t. verus* that has been  
604 attributed to past infections with SIV or SIV-like viruses [70]. Although we cannot  
605 speculate further given the nature of the data in this study, our findings add to the  
606 mounting evidence that chimpanzees have experienced long-lasting host-virus  
607 relationships with SIV-like viruses and that these relationships have been a critical  
608 process underpinning their evolution. More detailed investigations are needed on  
609 whether the positive selection in *P. t. elliotti* is due to past, recent, or ongoing infection  
610 with SIVcpz and/or related viruses.

## 611 **Signatures of selection across variable habitats**

612 Cameroon is also a uniquely positioned 'natural laboratory' to examine the  
613 relative contributions of neutral evolutionary forces versus natural selection in the  
614 evolution of many animals, including chimpanzees. In addition to being home to the  
615 Sanaga River, a well-known biogeographic boundary for many species, the country is  
616 exceptionally ecologically diverse. We speculate that the area is important for  
617 understanding how habitat variation and behavioral diversity may impact chimpanzee  
618 evolution. The Congo Basin Forest in the south, the Gulf of Guinea Forest in the west,  
619 and the Sahelian habitats in the north of Cameroon all converge and interdigitate to  
620 form a unique ecotone habitat composed of open woodland, savanna, and riparian  
621 forest [71]. This ecotone is a known engine of diversification for many species [72-78].  
622 Differences between *P. t. elliotti* and *P. t. troglodytes* have been linked with habitat  
623 variation across Cameroon [62], which suggests a possible role of local adaptation in  
624 their genetic differentiation. Finally, there is a further genetic distinction within *P. t. elliotti*  
625 itself, with one gene pool associated with the mountainous rainforest in western

626 Cameroon and the other with the ecotone in central Cameroon [24] (**Fig. 1b**). Each  
627 gene pool has a unique ecological niche [42, 79] with marked differences in key  
628 socioecological variables, including sex-specific differences in community structure [80]  
629 and dietary preferences [81].

630 We observed compelling evidence for positive selection that distinguished *P. t.*  
631 *troglodytes* from *P. t. ellioti* across this contact zone. We also found evidence of  
632 diversifying selection that distinguished *P. t. ellioti* populations that occupy different  
633 niches [42], which adds strength to our previous findings that both allopatric divergence  
634 due to genetic drift and environmentally-mediated local adaptation contribute to  
635 sustaining the prolonged separation of these two subspecies across this narrow contact  
636 zone between them. In particular, we found 246 genes involved in cellular, metabolic,  
637 and developmental processes were associated with one or more of the 31  
638 environmental predictor variables. Genes with the most divergent allele frequencies  
639 were associated with latitudinal variation and separate *P. t. ellioti* from *P. t. troglodytes*.  
640 We detected an additional more subtle signal of positive selection among *P. t. ellioti*  
641 chimpanzees located in western Cameroon's mountainous, forested regions compared  
642 to the population inhabiting central Cameroon's drier ecotone forests. Environmentally  
643 driven pressures between habitats shape adaptive variation, especially between  
644 rainforest and ecotone habitats. Chimpanzees in these two different habitat types were  
645 previously identified as distinctive ecological populations occupying unique niches [42,  
646 79]. The two ecological populations also exhibit distinctive differences in diet and  
647 nesting preferences [81, 82], key elements of chimpanzee cultural diversity.

648        Thus, multiple phenotypic axes appear to be under environmentally mediated  
649        selection that can be linked to habitat variation and variation in chimpanzee  
650        socioecology. Genes under environmentally mediated selection associated with  
651        neurological development (e.g., *LINGO2*) could be shaped by selective pressures linked  
652        to the development of cultural traits in diverse habitats [37], while those associated with  
653        diet and metabolism are likely shaped by pressures related to fruit availability and  
654        seasonality [81]. One of the most compelling findings of our study is the identification of  
655        24 genes related to digestion and metabolism with the strongest signals of  
656        environmentally-mediated selection, including *ACAT2*, *PLCL2*, and *IP6K2*, which  
657        present promising avenues for future research.

658        This study adds to the emerging evidence that neutral evolutionary forces alone  
659        cannot explain the prolonged persistence of the separation of *P. t. ellioti* from *P. t.*  
660        *troglodytes* across the narrow contact zone between them. Local adaptation to  
661        prevailing conditions has led to divergence in sets of genes important in immune  
662        response, neurological development, behavior, and dietary function. Together, these  
663        findings suggest that local adaptation, notably to varying pathogen pressure and  
664        different habitat types, has shaped chimpanzee subspecies differentiation in Cameroon,  
665        and likely across their broad range. Future studies exploring how these genetic  
666        differences map to phenotypic differences in wild populations are needed to better  
667        understand precisely which traits — particularly those associated with pathogen  
668        defense, diet, social organization, and other aspects of chimpanzee cultural diversity —  
669        provide for local adaptation and divergence among chimpanzee populations across this  
670        region.

671

## 672 Materials and Methods

### 673 Captive chimpanzee genomes

#### 674 Sequencing and read mapping

675 Our captive chimpanzee genomic dataset includes 24 previously sequenced [16]  
676 and 8 new chimpanzee genomes from Cameroon, representing all four subspecies: 4 *P.  
677 t. verus*, 10 *P. t. elliotti*, 12 *P. t. troglodytes*, and 6 *P. t. schweinfurthii* (**Table S1**). These  
678 eight genomes were sequenced using established methods [16] and deposited in  
679 GenBank. Details on the samples, the estimated origins of the captive chimpanzees  
680 [83], and GenBank accession numbers are in **Fig S1** and **Table S1**. We mapped raw  
681 sequencing reads against the chimpanzee reference genome Pan\_troglodytes-2.1.4  
682 (*panTro4*; [https://www.ncbi.nlm.nih.gov/assembly/GCF\\_000001515.6/](https://www.ncbi.nlm.nih.gov/assembly/GCF_000001515.6/)) using BWA-  
683 MEM v0.7.12 [84] with default parameters. After removing PCR duplicates using  
684 PICARD v1.119 (<https://broadinstitute.github.io/picard/index.html>), we called variants  
685 using FREEBAYES v0.9.20 [85]. After filtering, 12,754,225 high-quality bi-allelic SNPs  
686 on the autosomes were retained.

#### 687 Genome scans for signals of selection

688 We divided SNP datasets into a 'Western lineage' (*P. t. verus* & *P. t. elliotti*;  $n=15$ )  
689 and 'Central/Eastern lineage' (*P. t. troglodytes* & *P. t. schweinfurthii*;  $n=17$ ). We applied  
690 two selection scan methods, cross-population extended haplotype homozygosity (XP-  
691 EHH) [86] and integrated haplotype score (iHS) [87] to detect sweeps using hapbin  
692 v1.2.0 [88]. Since both tests require haplotypes, we phased the whole-genome SNP

693 datasets (12,754,225 SNPs) with SHAPEIT v2.r837 [89] following established methods  
694 [18]. Genetic maps for *panTro4* were provided by de Manuel & Kuhlwilm *et al.* [18] and  
695 Auton & Feldel-Alon *et al.* [90]. iHS calculations used SNPs with a minor allele  
696 frequency (MAF) over 5%. We determined the ancestral state of each allele using the 6-  
697 primate EPO alignment ([ftp://ftp.ensembl.org/pub/release-80/fasta/ancestral\\_alleles/](ftp://ftp.ensembl.org/pub/release-80/fasta/ancestral_alleles/))  
698 [91, 92]. After phasing, ancestral allele assignment, and MAF filtering we used  
699 4,577,055 SNPs in the Western lineage and 6,475,338 SNPs in the Central/Eastern  
700 lineage for iHS. XP-EHH scores compared both lineages using 12,450,633 SNPs, and  
701 the results were normalized across the genome.

## 702 **Defining population-informative neutral SNPs**

703 Using normalized XP-EHH and iHS values, we identified SNPs expected to  
704 follow neutral evolution that met the following criteria: (i) a *p*-value of > 0.05, (ii) absent  
705 from the top 1% genomic regions under selection (see *Defining genomic ‘outlier’ regions*  
706 *in captive chimpanzees*), (iii) be located >10kb from a gene, and (iv) be in linkage  
707 equilibrium. Using these parameters, we defined 147,700 neutral SNPs reflecting  
708 chimpanzee population structure. We annotated these using the Variant Effect Predictor  
709 (VEP) v82 and the UpDownDistance plugin [93].

## 710 **Defining genomic ‘outlier’ regions**

711 To understand the amount of selection on the genome, we considered numbers  
712 of base pairs under selection (magnitude) and the size of regions affected (genome  
713 space). We employed iHS [87] and XP-EHH [86] to detect signatures of local positive  
714 selection. Both assume that long-range haplotypes remain unaffected by recombination,  
715 signifying natural selection even with small datasets [43, 94]. They are also

716 complementary: while iHS detects partial sweeps, XP-EHH identifies near-fixation  
717 events. Following Pickrell *et al.* [43], chromosomes were split into 100kb non-  
718 overlapping windows, and the fraction of SNPs with  $|iHS| > 2$  and the maximum XP-  
719 EHH was used as a test statistic. We analyzed the fraction of SNPs with  $|iHS| > 2$  and  
720 the maximum XP-EHH per window. We turned these into empirical *p*-values by binning  
721 windows by SNP count, with iHS dropping windows with < 100 SNPs. Each window's  
722 statistic value was compared against others in its bin to determine an empirical *p*-value.  
723 All bins were then sorted by this *p*-value. The top 1% of each test statistic was noted.  
724 'Outlier regions' were windows in this 1% (*p*-value < 0.01). Adjacent windows were  
725 merged, retaining the smallest *p*-value.

## 726 **Characterizing genomic regions under selection**

727 As XP-EHH and iHS are complementary, we analyzed the 1% tail of each test  
728 merging adjacent windows. Windows were extended by 50kb on either side and  
729 annotated for gene content using Ensembl's BioMart [95], including protein-coding  
730 genes, pseudogenes, and RNA coding genes. Genes within outlier regions were  
731 considered candidate genes. We tested whether these genomic regions carry certain  
732 types of gene content more often than expected by chance by randomly selecting  
733 regions equivalent in length and annotating them as described above. We repeated this  
734 process 10 times for the Western and Central/Eastern populations, respectively. We  
735 counted the number of protein coding genes, non-coding RNAs, and pseudogenes in  
736 the real and randomized datasets. We then calculated mean and standard deviation for  
737 each and performed a one-sample t-test to determine significance.

738 **Functional annotation and enrichment analysis of whole-genome**  
739 **datasets**

740 We used DAVID Bioinformatics Resources v6.8 [44] to annotate candidate genes  
741 and perform an enrichment analysis with default functional annotations (GO terms,  
742 KEGG pathways, protein domains). We concentrated on the ‘functional annotation  
743 clustering’ function using the highest classification stringency and adjusted the  
744 enrichment thresholds for EASE to 0.05, reducing non-significant term inclusion. This  
745 clustering reduces redundancy by grouping similar annotations. Clusters received a  
746 Group Enrichment Score based on their *p*-value, ranking their biological importance.  
747 High scores likely mean lower *p*-values for annotation members [44]. We omitted  
748 windows found in both Western and Central/Eastern lineages, analyzing them  
749 separately. We set a background gene population as the entire chimpanzee genome, as  
750 recommended for genome-wide studies [44].

751 **Wild chimpanzee SNP genotyping, population history, and**  
752 **selection analysis**

753 **Fecal sample collection, DNA extraction, and quantification**

754 We sampled wild, non-habituated chimpanzee populations using non-invasive  
755 methods during a series of field studies from 2003 to 2015 spanning remote forested  
756 regions of Cameroon (**Fig. 1b**). Sampling occurred in protected and unprotected areas,  
757 as detailed in **Table S6**. Chimpanzee fecal samples were collected and stored following  
758 established protocols [24]. All samples were transported from Cameroon to the United  
759 States in full compliance with the Convention of International Trade in Endangered

760 Species of Wild Fauna and Flora (CITES), the Centers for Disease Control (CDC)  
761 export and import regulations, and with approval from the Government of Cameroon.

762 Following established protocols [24], DNA was extracted from fecal samples with  
763 the QIAamp DNA Stool Mini Kit (Qiagen). Due to the low proportion of endogenous  
764 DNA in fecal gDNA extracts [96, 97], samples were sometimes extracted up to six times  
765 to ensure enough chimpanzee DNA for sequencing processes. The concentration of  
766 endogenous DNA was measured via quantitative real-time PCR using the Quantifiler™  
767 Human DNA Quantification Kit (Applied Biosystems) and methods from prior studies  
768 [24].

### 769 **SNP ascertainment, library preparation, DNA capture enrichment, and** 770 **sequencing**

771 We genotyped 9,986 SNPs of wild chimpanzees from Cameroon, chosen from  
772 the larger set of 12,450,633 SNPs identified in the captive chimpanzee genome dataset.  
773 This selection comprised: (i) population informative neutral SNPs (n=3,492) randomly  
774 selected 147,700 neutral SNPs defined in the whole-genome dataset from above; (ii)  
775 'outlier' SNPs (n=6,494) identified through iHS or xpEHH tests as being in the top 1%  
776 for selection signals and within or 10k bp up- or down- stream of a known gene; and, (iii)  
777 SNPs in genes involved in immune response, disease resistance, and dietary  
778 adaptation in humans (n=20) [98, 99]. For each targeted SNP, we designed two 80  
779 nucleotide biotinylated RNA probes, overlapping by 20bp, to create 100bp windows  
780 around each SNP using the panTro4 chimpanzee reference genome. After rigorous  
781 filtration using the Arbor Biosciences BLAST pipeline, we finalized a bait-set of 19,974  
782 probes, assigning one or two probes to each SNP based on the outcome of the  
783 stringent filtering process.

784 gDNA samples were prepared in clean facilities at Arbor Biosciences to prevent  
785 contamination. DNA was quantified, sonicated, and size-selected for around 300nt  
786 fragment lengths. Samples were converted to sequencing libraries via adapter ligation.  
787 They were index-amplified based on the DNA input amount. Up to 2 $\mu$ g of each library  
788 was then enriched using the myBaits system v3. Different enrichment and amplification  
789 protocols were applied depending on the DNA quantity in the starting extract. Libraries  
790 were combined for equal representation, sequenced on an Illumina HiSeq PE125 lane  
791 at HudsonAlpha, and protocols were consistent with studies on degraded or low  
792 endogenous DNA samples [96, 97].

### 793 **SNP calling and on-target read assessment**

794 We filtered sequence reads with the Illumina CASAVA-1.8 FASTQ Filter  
795 ([http://cancan.cshl.edu/labmembers/gordon/fastq\\_illumina\\_filter/](http://cancan.cshl.edu/labmembers/gordon/fastq_illumina_filter/)) and mapped them to  
796 the chimpanzee panTro4 genome using BWA-MEM. After removing PCR duplicates  
797 with PICARD, we called variants using FREEBAYES. We evaluated DNA capture  
798 enrichment and sequencing for the raw and filtered sequence reads using SAMtools  
799 v1.3.1 (101) and VCFtools v0.1.15 [100] following established methods (97) for all 192  
800 individuals. Using VCFtools, we filtered variant calls based on quality and coverage.  
801 SNPs with <5x coverage or quality score <30 were recorded as missing data [97].  
802 Positions with >60% missing data, a minor allele frequency below 5%, or individuals  
803 with >70% missing data were removed. This resulted in 7,878 SNPs from 112 samples,  
804 termed the '10k dataset'. Due to removing all Boumba Bek (BB) and Campo Ma'an (CP)  
805 samples, a second '1k dataset' was made with stricter site filtering, yielding 994 SNPs  
806 and 142 samples, which included two from CP but none from BB. We also removed

807 closely related and duplicate samples using the R package related [101] using the  
808 triadic likelihood method [102], resulting in 85 individuals in the ‘10k dataset’ and 108  
809 individuals in the ‘1k dataset.’

810 **Testing for isolation-by-environment and inferring population  
811 structure**

812 **S1 Text** provides full details on methods to test IDB, IBE and to infer population  
813 structure, hybridization, and demographic history. In brief, we examined IDB versus IBE  
814 using pairwise  $F_{ST}$  values between sampling locations using Arlequin v3.5 [103], while  
815 geographic distances were determined with the geosphere package in R [104], focusing  
816 on areas with more than one individual. Population structure was inferred by PCA and  
817 ADMIXTURE analysis [105], DISTRUCT v1.1 [106], CLUMPP v1.1.2 [107], with  
818 geographic without pre-assigned population labels using the SNPrelate package in R,  
819 focusing on ‘neutral’ SNPs identified from captive chimpanzee genomes. We mapped  
820 genetic clusters using TESS [108] and Ad-Mixer v1.0 [109], accounting for IDB. We  
821 calculated observed and expected heterozygosity using the adegenet package in R  
822 [110], identified potential hybrids using NEWHYBRIDS v1.0 [111] as implemented in the  
823 R packages *hybriddetective* [112] and *parallelnewhybrid* [113], and investigated  
824 demographic history using  $\delta\alpha\delta\iota$  [114] to model asymmetric migration patterns between  
825 *P. t. ellioti* and *P. t. troglodytes*.

826 Environmental data layers (**Table S7**) were compiled and analyzed to assess  
827 habitat suitability and IBE for chimpanzees in Cameroon and Nigeria. These layers,  
828 sourced from publicly available databases, included diverse variables such as  
829 topography, hydrography, climate, vegetation, moisture content, and tree cover. After

830 standardizing these layers to a 30-arcsecond resolution and converting them to the  
831 WGS84 coordinate system, the dataset underwent cross-correlation analysis to pinpoint  
832 environmental factors significantly influencing chimpanzee distribution (**Table S8**).

### 833 **Mapping genomic variation across habitats**

834 Using the R package *gradientForest* [50], we calculated associations between  
835 allele frequencies and environmental variation across suitable habitat. This extended  
836 random forest model identifies links between response variables (e.g., SNP allele  
837 frequencies) and spatial environmental factors [115] by iteratively processing datasets,  
838 assessing outliers and predictor significance. Gradient forests further apply regression  
839 to multiple responses, revealing genomic variation from environmental shifts. This can  
840 pinpoint areas of high intraspecific variation, subspecies transitions, or barriers  
841 separating genomic variation related to the environment [116]. Following established  
842 methods, we refined the environmental dataset (**Table S7**) to reduce noise and applied  
843 the gradient forest model [76].

844 We ran gradient forests on 7,878 SNP allele frequencies used as a response  
845 dataset, and 17 environmental variables as the predictors in our final model, including  
846 measures of temperature, precipitation, vegetation, surface moisture, and geographic  
847 features at the sampling locations. We ran 100 trees in our model, noting SNPs  
848 significantly associated with any environmental variable ( $R^2 > 0$ ) and the average  
849 regression of all associated SNPs. To assess model performance, we randomized the  
850 environmental data and ran 200 permutations of the model, creating a distribution of  $R^2$

851 and significant SNP associations. We then ran 200 permutations of the actual model,  
852 comparing these distributions. (**Fig. S25**).

### 853 **Detecting environmentally associated loci under selection**

854 In order to understand the degree to which environmentally driven natural  
855 selection may cause chimpanzees to be locally adapted to different habitats, we used  
856 latent factor mixed models implemented in the program LFMM v1.5 [117]. LFMM  
857 quantifies statistical associations between allele frequencies and environmental  
858 variables, accounts for underlying population genetic structure, and detects loci with  
859 stronger environmental correlations than population structure. We ran five MCMC  
860 replicates for all environmental variable with 25,000 burn-in steps, 100,000 iterations,  
861 and a latent factor of  $K=3$  from *a priori* knowledge of wild chimpanzee population  
862 structure in Cameroon (**Figs. S11, S12, S13, S14 S15, S16, S20 and S21**). We  
863 calculated median z-scores across runs and used them to calculate the genomic  
864 inflation factor ( $\lambda$ ) and adjusted  $p$ -values. To correct for multiple testing, we applied a  
865 conservative false discovery rate (FDR) of 0.1 using the Benjamini-Hochberg algorithm.  
866 We identified unique candidate SNPs linked to at least one environmental variable,  
867 presented via Manhattan plots using the *qqman* package [118].

868 Using outlier analysis with LFMM, we grouped highly correlated environmental  
869 variables together to create 'environmental groupings' (**Table S9**). These included:  
870 General Temperature (n=7), Temperature Range (n=2), Temperature Seasonality (n=2),  
871 Precipitation – Wet/Cold (n=4), Precipitation – Dry/Warm (n=4), Tree Cover (n=2),  
872 Vegetation Brownness (n=2), Vegetation Greenness (n=3), Surface Moisture Content  
873 (n=2), and Topography (n=3). To determine the degree to which types of environmental

874 variation may drive selection of different genomic regions, we identified panels of unique  
875 candidates from each 'environmental grouping.' We also analyzed the impact of  
876 multicollinearity of our environmental predictors on the LFMM results by correlating the  
877 degree of association between pairs of environmental predictors and the number of  
878 shared outlier SNPs, using a Mantel test in R. (**Table S8**).

## 879 **Enriched gene ontologies and KEGG pathways**

880 We identified candidate genes near candidate SNPs positions with Ensembl's  
881 BioMart tool [119, 120], including both complete and partial genes within these  
882 windows. We used the DAVID database [44] for annotation and enrichment analysis of  
883 candidate gene lists focusing on the 'Biological Processes' category of the 'Gene  
884 Ontology' database [121] and KEGG pathways [60] using a *p*-value threshold of 0.05  
885 and two different background populations of genes to control for potential bias since the  
886 SNPs assayed in wild chimpanzees were selected from a subset of those identified  
887 using whole-genome data from captive individuals. The first background we used was  
888 composed of the population of genes found outside regions under selection identified in  
889 the whole-genome sequencing data (**Fig 2a**). This resulted in a broad view of  
890 environmentally mediated selection in wild chimpanzees by including only genes in  
891 putatively neutral regions of the genome. The second background population of genes  
892 consisted of all genes assayed in wild chimpanzees, excluding environmental outliers.

893

894

## 895 Acknowledgments

896 We thank the government of Cameroon for permission to conduct this research.  
897 We thank the Congo Basin Institute, the International Institute for Tropical Agriculture,  
898 the Cameroon Biodiversity Association, the San Diego Zoo Wildlife Alliance, the Wildlife  
899 Conservation Society, and the World Wildlife Fund for their support in Cameroon. We  
900 thank Kevin Njabo, Beatrice Hahn, Martine Peeters, Louis Nkembi, and Amy  
901 Pokempner for their assistance in collecting fecal samples in Cameroon. We thank  
902 Felice Elefant for the use of her lab's 7500 Real-Time PCR System. We thank Alison  
903 Devault and Jacob Enk of Arbor Biosciences for assistance in the experimental design  
904 and execution of the wild chimpanzee DNA capture enrichment and sequencing as part  
905 of Arbor Biosciences' myReads services.

906

907

## 908 References

909

910 1. Coyne JA, Orr HA. *Speciation*. Sunderland, Mass.: Sinauer Associates; 2004. xiii, 545, 2 p. of  
911 plates p.

912 2. Nielsen R. Molecular Signatures of Natural Selection. *Annu Rev Genet*. 2005;39(1):197-218. doi:  
913 10.1146/annurev.genet.39.073003.112420.

914 3. Moritz C, Patton JL, Schneider CJ, Smith TB. Diversification of rainforest faunas: An integrated  
915 molecular approach. *Annu Rev Ecol Syst*. 2000;31(1):533-63. doi:  
916 doi:10.1146/annurev.ecolsys.31.1.533.

917 4. Sabeti PC, Schaffner SF, Fry B, Lohmueller J, Varilly P, Shamovsky O, et al. Positive natural  
918 selection in the human lineage. *Science*. 2006;312(5780):1614-20. doi: 10.1126/science.1124309

919 5. Hancock AM, Witonsky DB, Gordon AS, Eshel G, Pritchard JK, Coop G, Di Rienzo A.  
920 Adaptations to climate in candidate genes for common metabolic disorders. *PLoS Genet*.  
921 2008;4(2):e32. doi: 10.1371/journal.pgen.0040032.

922 6. Manel S, Holderegger R. Ten years of landscape genetics. *Trends Ecol Evol*. 2013;28(10):614-  
923 21. doi: 10.1016/j.tree.2013.05.012.

924 7. Novembre J, Galvani AP, Slatkin M. The Geographic Spread of the CCR5 Δ32 HIV-Resistance  
925 Allele. *PLoS Biol*. 2005;3(11):1954-62. doi: 10.1371/journal.pbio.0030339.

926 8. Hedrick PW. Population genetics of malaria resistance in humans. *Heredity*. 2011;107(4):283-  
927 304. doi: 10.1038/hdy.2011.16.

928 9. Tishkoff SA, Reed FA, Ranciaro A, Voight BF, Babbitt CC, Silverman JS, et al. Convergent  
929 adaptation of human lactase persistence in Africa and Europe. *Nature Genet*. 2007;39(1):31-40.  
930 doi: 10.1038/ng1946.

931 10. Fumagalli M, Moltke I, Grarup N, Racimo F, Bjerregaard P, Jørgensen ME, et al. Greenlandic  
932 Inuit show genetic signatures of diet and climate adaptation. *Science*. 2015;349(6254):1343-7.  
933 doi: doi:10.1126/science.aab2319.

934 11. Jarvis JP, Scheinfeldt LB, Soi S, Lambert C, Omberg L, Ferwerda B, et al. Patterns of Ancestry,  
935 Signatures of natural selection, and genetic association with stature in Western African Pygmies.  
936 *PLoS Genet*. 2012;8(4):e1002641. doi: 10.1371/journal.pgen.1002641.

937 12. Hancock AM, Witonsky DB, Ehler E, Alkorta-Aranburu G, Beall C, Gebremedhin A, et al. Human  
938 adaptations to diet, subsistence, and ecoregion are due to subtle shifts in allele frequency. *Proc  
939 Natl Acad Sci USA*. 2010;107(supplement\_2):8924-30. doi: doi:10.1073/pnas.0914625107.

940 13. Bhandari S, Zhang X, Cui C, Yangla, Liu L, Ouzhuluobu, et al. Sherpas share genetic variations  
941 with Tibetans for high-altitude adaptation. *Mol Genet Genomic Med*. 2017;5(1):76-84. doi:  
942 10.1002/mgg3.264.

943 14. Hanaoka M, Droma Y, Basnyat B, Ito M, Kobayashi N, Katsuyama Y, et al. Genetic variants in  
944 *EPAS1* contribute to adaptation to high-altitude hypoxia in Sherpas. *PLoS ONE*.  
945 2012;7(12):e50566. doi: 10.1371/journal.pone.0050566.

946 15. Scheinfeldt LB, Soi S, Thompson S, Ranciaro A, Woldemeskel D, Beggs W, et al. Genetic  
947 adaptation to high altitude in the Ethiopian highlands. *Genome Biol*. 2012;13(1):R1. doi:  
948 10.1186/gb-2012-13-1-r1.

949 16. Prado-Martinez J, Sudmant PH, Kidd JM, Li H, Kelley JL, Lorente-Galdos B, et al. Great ape  
950 genetic diversity and population history. *Nature*. 2013;499(7459):471-5. doi: 10.1038/nature12228

951 17. Xue YL, Prado-Martinez J, Sudmant PH, Narasimhan V, Ayub Q, Szpak M, et al. Mountain gorilla  
952 genomes reveal the impact of long-term population decline and inbreeding. *Science*.  
953 2015;348(6231):242-5. doi: 10.1126/science.aaa3952. PubMed PMID: WOS:000352613700048.

954 18. de Manuel M, Kuhlwilm M, Frandsen P, Sousa VC, Desai T, Prado-Martinez J, et al. Chimpanzee  
955 genomic diversity reveals ancient admixture with bonobos. *Science*. 2016;354(6311):477-81. doi:  
956 10.1126/science.aag2602.

957 19. Cagan A, Theunert C, Laayouni H, Santpere G, Pybus M, Casals F, et al. Natural selection in the  
958 great apes. *Mol Biol Evol.* 2016;33(12):3268-83. doi: 10.1093/molbev/msw215. PubMed PMID:  
959 WOS:000387925300021.

960 20. Nater A, Mattle-Greminger MP, Nurcahyo A, Nowak MG, de Manuel M, Desai T, et al. Morphometric, behavioral, and genomic evidence for a new orangutan species. *Current Biol.*  
961 2017;27(22):3487-98.e10. doi: 10.1016/j.cub.2017.09.047.

962 21. Anthony NM, Johnson-Bawe M, Jeffery K, Clifford SL, Abernethy KA, Tutin CE, et al. The role of  
963 Pleistocene refugia and rivers in shaping gorilla genetic diversity in central Africa. *Proc Natl Acad  
964 Sci USA.* 2007;104(51):20432-6. Epub 2007/12/14. doi: 10.1073/pnas.0704816105.

965 22. Gonder MK, Oates JF, Disotell TR, Forstner MR, Morales JC, Melnick DJ. A new west African  
966 chimpanzee subspecies? *Nature.* 1997;388(6640):337. doi: 10.1038/41005.

967 23. Gonder MK, Disotell TR, Oates JF. New genetic evidence on the evolution of chimpanzee  
968 populations, and implications for taxonomy. *Int J Primatol.* 2006;27(4):1103-27. doi:  
969 10.1007/s10764-006-9063-y.

970 24. Mitchell MW, Locatelli S, Ghobrial L, Pokempner AA, Sesink Clee PR, Abwe EE, et al. The  
971 population genetics of wild chimpanzees in Cameroon and Nigeria suggests a positive role for  
972 selection in the evolution of chimpanzee subspecies. *BMC Evol Biol.* 2015;15:3. doi:  
973 10.1186/s12862-014-0276-y.

974 25. Mattle-Greminger MP, Bilgin Sonay T, Nater A, Pybus M, Desai T, de Valles G, et al. Genomes  
975 reveal marked differences in the adaptive evolution between orangutan species. *Genome Biol.*  
976 2018;19(1):193. doi: 10.1186/s13059-018-1562-6.

977 26. Rodrigues MF, Kern AD, Ralph PL. Shared evolutionary processes shape landscapes of genomic  
978 variation in the great apes. *Genet.* 2024;226(4):iya006. doi: 10.1093/genetics/iya006.

979 27. Fontseré C, Kuhlwilm M, Morcillo-Suarez C, Alvarez-Estepe M, Lester JD, Gratton P, et al.  
980 Population dynamics and genetic connectivity in recent chimpanzee history. *Cell Genom.*  
981 2022;2(6). doi: 10.1016/j.xgen.2022.100133.

982 28. Sharp PM, Plenderleith LJ, Hahn BH. Ape Origins of Human Malaria. *Annu Rev Microbiol.*  
983 2020;74(1):39-63. doi: 10.1146/annurev-micro-020518-115628.

984 29. Leendertz SAJ, Wich SA, Ancrenaz M, Bergl RA, Gonder MK, Humle T, Leendertz FH. Ebola in  
985 great apes – current knowledge, possibilities for vaccination, and implications for conservation  
986 and human health. *Mammal Rev.* 2016;n/a-n/a. doi: 10.1111/mam.12082.

987 30. Locatelli S, McKean KA, Sesink Clee PR, Gonder MK. The Evolution of Resistance to Simian  
988 Immunodeficiency Virus (SIV): A Review. *Int J Primatol.* 2014;35(2):349-75. doi: 10.1007/s10764-  
989 014-9763-7.

990 31. Bibollet-Ruche F, Russell RM, Liu W, Stewart-Jones GBE, Sherrill-Mix S, Li Y, et al. CD4  
991 receptor diversity in chimpanzees protects against SIV infection. *Proc Natl Acad Sci USA.*  
992 2019;116(8):3229-38. doi: 10.1073/pnas.1821197116.

993 32. Schmidt JM, de Manuel M, Marques-Bonet T, Castellano S, Andrés AM. The impact of genetic  
994 adaptation on chimpanzee subspecies differentiation. *PLoS Genet.* 2019;15(11):e1008485. doi:  
995 10.1371/journal.pgen.1008485.

996 33. Pawar H, Ostridge HJ, Schmidt JM, Andrés AM. Genetic adaptations to SIV across chimpanzee  
997 populations. *PLoS Genet.* 2022;18(8):e1010337. doi: 10.1371/journal.pgen.1010337.

998 34. Locatelli S, Harrigan RJ, Sesink Clee PR, Mitchell MW, McKean KA, Smith TB, Gonder MK. Why  
999 are Nigeria-Cameroon Chimpanzees (*Pan troglodytes elliotti*) free of SIVcpz infection? *PLoS  
1000 ONE.* 2016;11(8):e0160788. doi: 10.1371/journal.pone.0160788.

1001 35. Prince AM, Brotman B, Lee D-H, Andrus L, Valinsky J, Marx P. Lack of evidence for HIV Type 1-  
1002 related SIVcpz infection in captive and wild chimpanzees (*Pan troglodytes verus*) in West Africa.  
1003 AIDS Res Hum Retroviruses. 2002;18(9):657-60. doi: 10.1089/088922202760019356. PubMed  
1004 PMID: 12079561.

1005 36. Leendertz SAJ, Locatelli S, Boesch C, Kücherer C, Formenty P, Liegeois F, et al. No evidence for  
1006 transmission of SIVwrc from western red colobus monkeys (*Piliocolobus badius badius*) to wild  
1007 west african chimpanzees (*Pan troglodytes verus*) despite high exposure through hunting. *BMC  
1008 Microbiol.* 2011;11(1):24. doi: 10.1186/1471-2180-11-24.

1009 37. Kalan AK, Kulik L, Arandjelovic M, Boesch C, Haas F, Dieguez P, et al. Environmental variability  
1010 supports chimpanzee behavioural diversity. *Nat Commun.* 2020;11(1):4451. doi: 10.1038/s41467-  
1011 020-18176-3.

1012

1013 38. Wessling EG, Deschner T, Mundry R, Pruetz JD, Wittig RM, Kühl HS. Seasonal Variation in  
1014 Physiology Challenges the Notion of Chimpanzees (*Pan troglodytes verus*) as a Forest-Adapted  
1015 Species. *Front Ecol Evol.* 2018;6. doi: 10.3389/fevo.2018.00060.

1016 39. Boesch C, Kalan AK, Mundry R, Arandjelovic M, Pika S, Dieguez P, et al. Chimpanzee  
1017 ethnography reveals unexpected cultural diversity. *Nat Hum Behav.* 2020;4(9):910-6. doi:  
1018 10.1038/s41562-020-0890-1.

1019 40. Kühl HS, Boesch C, Kulik L, Haas F, Arandjelovic M, Dieguez P, et al. Human impact erodes  
1020 chimpanzee behavioral diversity. *Science.* 2019;363(6434):1453-5. doi:  
1021 doi:10.1126/science.aau4532.

1022 41. Stumpf R. Chimpanzees and Bonobos, Diversity within and between species. In: Campbell CJ,  
1023 Fuentes A, MacKinnon KC, Panger M, Bearder SK, editors. *Primates in Perspective.* New York:  
1024 Oxford University Press; 2007. p. 321-44.

1025 42. Sesink Clee PR, Abwe EE, Ambahe RD, Anthony NM, Fotso R, Locatelli S, et al. Chimpanzee  
1026 genetic structure in Cameroon and Nigeria is associated with habitat variation that may be lost  
1027 under climate change. *BMC Evolutionary Biology.* 2015;15:2. doi: 10.1186/s12862-014-0275-z.

1028 43. Pickrell JK, Coop G, Novembre J, Kudaravalli S, Li JZ, Absher D, et al. Signals of recent positive  
1029 selection in a worldwide sample of human populations. *Genome Res.* 2009;19(5):826-37. doi:  
1030 10.1101/gr.087577.108.

1031 44. Huang DW, Sherman BT, Lempicki RA. Systematic and integrative analysis of large gene lists  
1032 using DAVID bioinformatics resources. *Nat Protoc.* 2009;4:44. doi: 10.1038/nprot.2008.211.

1033 45. Villadangos JA. Presentation of antigens by MHC class II molecules: getting the most out of  
1034 them. *Mol Immunol.* 2001;38(5):329-46. doi: 10.1016/s0026-2850(01)00069-4.

1035 46. Pasquale EB. EPH receptor signalling casts a wide net on cell behaviour. *Nat Rev Mol Cell Biol.*  
1036 2005;6(6):462-75. doi: 10.1038/nrm1662. PubMed PMID: WOS:000229629100013.

1037 47. Kania A, Klein R. Mechanisms of ephrin-Eph signalling in development, physiology and disease.  
1038 *Nat Rev Mol Cell Biol.* 2016;17(4):240-56. doi: 10.1038/nrm.2015.16.

1039 48. Aihara E, Engevik KA, Montrose MH. Trefoil Factor Peptides and Gastrointestinal Function. *Annu  
1040 Rev Physiol.* 2017; 79: 357-380.

1041 49. Weinberg A, Jin G, Sieg S, McCormick T. The Yin and Yang of Human Beta-Defensins in Health  
1042 and Disease. *Front Immunol.* 2012;3(294). doi: 10.3389/fimmu.2012.00294.

1043 50. Ellis N, Smith SJ, Pitcher CR. Gradient forests: calculating importance gradients on physical  
1044 predictors. *Ecol.* 2012;93(1):156-68. doi: 10.1890/11-0252.1.

1045 51. Hansen TH, Bouvier M. MHC class I antigen presentation: learning from viral evasion strategies.  
1046 *Nat Rev Immunol.* 2009;9(7):503-13. doi: 10.1038/nri2575.

1047 52. Luo Y, Jacobs EY, Greco TM, Mohammed KD, Tong T, Keegan S, et al. HIV–host interactome  
1048 revealed directly from infected cells. *Nat Microbiol.* 2016;1(7):16068. doi:  
1049 10.1038/nmicrobiol.2016.68.

1050 53. Abitew AM, Sobti RC, Sharma VL, Wanchu A. Analysis of transporter associated with antigen  
1051 presentation (TAP) genes polymorphisms with HIV-1 infection. *Mol Cel Biochem.* 2020;464(1):65-  
1052 71. doi: 10.1007/s11010-019-03649-x.

1053 54. Fagerberg L, Hallström BM, Oksvold P, Kampf C, Djureinovic D, Odeberg J, et al. Analysis of the  
1054 Human Tissue-specific Expression by Genome-wide Integration of Transcriptomics and Antibody-  
1055 based Proteomics \*. *Mol Cell Proteomics.* 2014;13(2):397-406. doi: 10.1074/mcp.M113.035600.

1056 55. Williams SM, An JY, Edson J, Watts M, Murigneux V, Whitehouse AJO, et al. An integrative  
1057 analysis of non-coding regulatory DNA variations associated with autism spectrum disorder. *Mol  
1058 Psychiatry.* 2019;24(11):1707-19. doi: 10.1038/s41380-018-0049-x.

1059 56. Eusebi PG, Cortés O, Carleos C, Dunner S, Cañon J. Detection of selection signatures for  
1060 agonistic behaviour in cattle. *J Anim Breed Genet.* 2018;135(3):170-7. doi: 10.1111/jbg.12325.

1061 57. Parini P, Davis M, Lada AT, Erickson SK, Wright TL, Gustafsson U, et al. ACAT2 Is Localized to  
1062 Hepatocytes and Is the Major Cholesterol-Esterifying Enzyme in Human Liver. *Circulation.*  
1063 2004;110(14):2017-23. doi: 10.1161/01.CIR.0000143163.76212.0B.

1064 58. Oue K, Zhang J, Harada-Hada K, Asano S, Yamawaki Y, Hayashiuchi M, et al. Phospholipase C-  
1065 related Catalytically Inactive Protein Is a New Modulator of Thermogenesis Promoted by  $\beta$ -  
1066 Adrenergic Receptors in Brown Adipocytes. *J Biol Chem.* 2016;291(8):4185-96. doi:  
1067 10.1074/jbc.M115.705723.

1068 59. Jostins L, Ripke S, Weersma RK, Duerr RH, McGovern DP, Hui KY, et al. Host–microbe  
1069 interactions have shaped the genetic architecture of inflammatory bowel disease. *Nature*.  
1070 2012;491(7422):119–24. doi: 10.1038/nature11582.

1071 60. Kanehisa M, Goto S. KEGG: Kyoto Encyclopedia of Genes and Genomes. *Nucleic Acids Res*.  
1072 2000;28(1):27–30. doi: 10.1093/nar/28.1.27.

1073 61. Kanehisa M. Toward understanding the origin and evolution of cellular organisms. *Protein Sci*.  
1074 2019;28(11):1947–51. doi: 10.1002/pro.3715.

1075 62. Mitchell MW, Locatelli S, Sesink Clee PR, Thomassen HA, Gonder MK. Environmental variation  
1076 and rivers govern the structure of chimpanzee genetic diversity in a biodiversity hotspot. *BMC  
1077 Evol Biol*. 2015;15:1. doi: 10.1186/s12862-014-0274-0.

1078 63. Gao F, Bailes E, Robertson DL, Chen Y, Rodenburg CM, Michael SF, et al. Origin of HIV-1 in the  
1079 chimpanzee *Pan troglodytes troglodytes*. *Nature*. 1999;397(6718):436–41. doi: 10.1038/17130.

1080 64. Keele BF, Van Heuverswyn F, Li Y, Bailes E, Takehisa J, Santiago ML, et al. Chimpanzee  
1081 reservoirs of pandemic and nonpandemic HIV-1. *Science*. 2006;313(5786):523–6. doi:  
1082 10.1126/science.1126531

1083 65. Van Heuverswyn F, Li Y, Neel C, Bailes E, Keele BF, Liu W, et al. SIV infection in wild gorillas.  
1084 *Nature*. 2006;444(7116):164–. doi: 10.1038/444164a.

1085 66. D'arc M, Ayouba A, Esteban A, Learn GH, Boué V, Liegeois F, et al. Origin of the HIV-1 group O  
1086 epidemic in western lowland gorillas. *Proc Natl Acad Sci USA*. 2015;112(11):E1343–E52. doi:  
1087 doi:10.1073/pnas.1502022112.

1088 67. Bailes E, Gao F, Bibollet-Ruche F, Courgnaud V, Peeters M, Marx PA, et al. Hybrid origin of SIV  
1089 in chimpanzees. *Science*. 2003;300(5626):1713–. doi: doi:10.1126/science.1080657.

1090 68. Sharp PM, Shaw GM, Hahn BH. Simian Immunodeficiency virus infection of chimpanzees. *J  
1091 Virol*. 2005;79(7):3891–902. doi: 10.1128/JVI.79.7.3891-3902.2005.

1092 69. Rudicell RS, Holland Jones J, Wroblewski EE, Learn GH, Li Y, Robertson JD, et al. Impact of  
1093 Simian Immunodeficiency Virus infection on chimpanzee population dynamics. *PLoS Pathog*.  
1094 2010;6(9):e1001116. doi: 10.1371/journal.ppat.1001116

1095 70. de Groot NG, Otting N, Doxiadis GGM, Balla-Jhagjhoorsingh SS, Heeney JL, van Rood JJ, et al.  
1096 Evidence for an ancient selective sweep in the MHC class I gene repertoire of chimpanzees. *Proc  
1097 Natl Acad Sci USA*. 2002;99(18):11748–53. doi: 10.1073/pnas.182420799.

1098 71. Maisels F. Mbam Djerem National Park, Cameroon: at the forest's edge. *Canopée*. 2005;27:2–6.

1099 72. Smith TB, Wayne RK, Girman DJ, Bruford MW. A role for ecotones in generating rainforest  
1100 biodiversity. *Science*. 1997;276(5320):1855–7. doi: 10.1126/science.276.5320.1855.

1101 73. Simard F, Ayala D, Kamdem G, Pombi M, Etouna J, Ose K, et al. Ecological niche partitioning  
1102 between *Anopheles gambiae* molecular forms in Cameroon: the ecological side of speciation.  
1103 *BMC Ecol*. 2009;9(1):17. doi:10.1186/1472-6785-9-17.

1104 74. Smith TB, Thomassen HA, Freedman AH, Sehgal RNM, Buermann W, Saatchi S, et al. Patterns  
1105 of divergence in the olive sunbird *Cyanomitra olivacea* (Aves: Nectariniidae) across the African  
1106 rainforest-savanna ecotone. *Biol J Linnean Soc*. 2011;103(4):821–35. doi: 10.1111/j.1095-  
1107 8312.2011.01674.x.

1108 75. Freedman AH, Thomassen HA, Buermann W, Smith TB. Genomic signals of diversification along  
1109 ecological gradients in a tropical lizard. *Mol Ecol*. 2010;19(17):3773–88. doi: 10.1111/j.1365-  
1110 294X.2010.04684.x.

1111 76. Zhen Y, Harrigan RJ, Ruegg KC, Anderson EC, Ng TC, Lao SRN, et al. Genomic divergence  
1112 across ecological gradients in the Central African rainforest songbird (*Andropadus virens*). *Mol  
1113 Ecol*. 2017;26(19):4966–77. doi: 10.1111/mec.14270.

1114 77. Morgan K, Mboumba J-F, Ntie S, Mickala P, Miller CA, Zhen Y, et al. Precipitation and vegetation  
1115 shape patterns of genomic and craniometric variation in the central African rodent *Praomys  
1116 misonnei*. *Proc Biol Sci B*. 2020;287(1930):20200449. doi: doi:10.1098/rspb.2020.0449.

1117 78. Freedman AH, Harrigan RJ, Zhen Y, Hamilton AM, Smith TB. Evidence for ecotone speciation  
1118 across an African rainforest-savanna gradient. *Mol Ecol*. 2023;32(9):2287–300. doi:  
1119 10.1111/mec.16867.

1120 79. Abwe EE, Morgan BJ, Tchiengue B, Kentatchime F, Doudja R, Ketchen ME, et al. Habitat  
1121 differentiation among three Nigeria–Cameroon chimpanzee (*Pan troglodytes elliotti*) populations.  
1122 *Ecol Evol*. 2019;9(3):1489–500. doi: 10.1002/ee.3.4871.

1123 80. Mitchell MW, Locatelli S, Abwe EE, Ghobrial L, Gonder MK. Male-driven differences in  
1124 chimpanzee (*Pan troglodytes*) population genetic structure across three habitats in Cameroon  
1125 and Nigeria. *Int J Primatol.* 2018;39(4):581-601. doi: 10.1007/s10764-018-0053-7.

1126 81. Abwe EE, Morgan BJ, Doudja R, Kentatchime F, Mba F, Dadjo A, et al. Dietary ecology of the  
1127 Nigeria–Cameroon chimpanzee (*Pan troglodytes ellioti*). *Int J Primatol.* 2020;41(1):81-104. doi:  
1128 10.1007/s10764-020-00138-7.

1129 82. Abwe EE. Linking behavioral diversity with genetic and ecological variation in the Nigeria-  
1130 Cameroon chimpanzee (*Pan troglodytes ellioti*): Drexel University; 2018.

1131 83. Ghobrial L, Lankester F, Kiyang JA, Akih AE, de Vries S, Fotso R, et al. Tracing the origins of  
1132 rescued chimpanzees reveals widespread chimpanzee hunting in Cameroon. *BMC Ecol.*  
1133 2010;10(1):2. doi: 10.1186/1472-6785-10-2.

1134 84. Li H. Aligning sequence reads, clone sequences and assembly contigs with BWA-MEM.  
1135 arXiv:1303.3997v1 [q-bio.GN]. 2013. doi: 10.48550/arXiv.1303.3997

1136 85. Garrison E, Marth G. Haplotype-based variant detection from short-read sequencing. ArXiv e-  
1137 prints [Internet]. 2012 July 01, 2012. Available from:  
1138 <https://ui.adsabs.harvard.edu/#abs/2012arXiv1207.3907G>.

1139 86. Sabeti PC, Varilly P, Fry B, Lohmueller J, Hostetter E, Cotsapas C, et al. Genome-wide detection  
1140 and characterization of positive selection in human populations. *Nature.* 2007;449:913. doi:  
1141 10.1038/nature06250

1142 87. Voight BF, Kudaravalli S, Wen X, Pritchard JK. A Map of Recent Positive Selection in the Human  
1143 Genome. *PLoS Biol.* 2006;4(3):e72. doi: 10.1371/journal.pbio.0040072.

1144 88. Maclean CA, Hong NPC, Prendergast JGD. hapbin: An Efficient Program for Performing  
1145 Haplotype-Based Scans for Positive Selection in Large Genomic Datasets. *Mol Biol Evol.*  
1146 2015;32(11):3027-9. doi: 10.1093/molbev/msv172.

1147 89. Delaneau O, Marchini J, Zagury J-F. A linear complexity phasing method for thousands of  
1148 genomes. *Nat Methods.* 2012;9:179. doi: 10.1038/nmeth.1785

1149 90. Auton A, Fledel-Alon A, Pfeifer S, Venn O, Ségurel L, Street T, et al. A fine-scale chimpanzee  
1150 genetic map from population sequencing. *Science.* 2012;336(6078):193-8. doi:  
1151 10.1126/science.1216872.

1152 91. Paten B, Herrero J, Beal K, Fitzgerald S, Birney E. Enredo and Pecan: Genome-wide mammalian  
1153 consistency-based multiple alignment with paralogs. *Genome Res.* 2008;18(11):1814-28. doi:  
1154 10.1101/gr.076554.108.

1155 92. Paten B, Herrero J, Fitzgerald S, Beal K, Flicek P, Holmes I, Birney E. Genome-wide nucleotide-  
1156 level mammalian ancestor reconstruction. *Genome Res.* 2008;18(11):1829-43. doi:  
1157 10.1101/gr.076521.108.

1158 93. McLaren W, Gil L, Hunt SE, Riat HS, Ritchie GRS, Thormann A, et al. The Ensembl Variant  
1159 Effect Predictor. *Genome Biol.* 2016;17:14. doi: 10.1186/s13059-016-0974-4.

1160 94. Huff CD, Harpending HC, Rogers AR. Detecting positive selection from genome scans of linkage  
1161 disequilibrium. *BMC Genomics.* 2010;11:9. doi: 10.1186/1471-2164-11-8. PubMed PMID:  
1162 WOS:000274642200001.

1163 95. Smedley D, Haider S, Durinck S, Pandini L, Provero P, Allen J, et al. The BioMart community  
1164 portal: an innovative alternative to large, centralized data repositories. *Nucleic Acids Res.*  
1165 2015;43(W1):W589-W98. doi: 10.1093/nar/gkv350.

1166 96. Perry GH, Marioni JC, Melsted P, Gilad Y. Genomic-scale capture and sequencing of  
1167 endogenous DNA from feces. *Mol Ecol.* 2010;19(24):5332-44. doi: 10.1111/j.1365-  
1168 294X.2010.04888.x.

1169 97. Hernandez-Rodriguez J, Arandjelovic M, Lester J, Filippo C, Weihmann A, Meyer M, et al. The  
1170 impact of endogenous content, replicates and pooling on genome capture from faecal samples.  
1171 *Mol Ecol Res.* 2018;18(2):319-33. doi: doi:10.1111/1755-0998.12728.

1172 98. Fan S, Hansen MEB, Lo Y, Tishkoff SA. Going global by adapting local: A review of recent  
1173 human adaptation. *Science.* 2016;354(6308):54-9. doi: 10.1126/science.aaf5098.

1174 99. Hancock AM, Witonsky DB, Ehler E, Alkorta-Aranburu G, Beall C, Gebremedhin A, et al. Human  
1175 adaptations to diet, subsistence, and ecoregion are due to subtle shifts in allele frequency. *Proc  
1176 Natl Acad Sci USA.* 2010;107(Supplement 2):8924-30. doi: 10.1073/pnas.0914625107.

1177 100. Danecek P, Auton A, Abecasis G, Albers CA, Banks E, DePristo MA, et al. The variant call format  
1178 and VCFtools. *Bioinformatics*. 2011;27(15):2156-8. doi: 10.1093/bioinformatics/btr330.

1179 101. Pew J, Muir PH, Wang J, Frasier TR. related: an R package for analysing pairwise relatedness  
1180 from codominant molecular markers. *Mol Ecol Res*. 2015;15(3):557-61. doi: 10.1111/1755-  
1181 0998.12323.

1182 102. Wang J. Triadic IBD coefficients and applications to estimating pairwise relatedness. *Genetical  
1183 Res*. 2007;89(3):135-53. doi: 10.1017/S0016672307008798.

1184 103. Excoffier L, Lischer HEL. Arlequin suite ver 3.5: A new series of programs to perform population  
1185 genetics analyses under Linux and Windows. *Mol Ecol Resources*. 2010;10(3):564-7. doi:  
1186 10.1111/j.1755-0998.2010.02847.x.

1187 104. Hijmans RJ. geosphere: Spherical Trigonometry. R package version 15-5. 2016. Available from:  
1188 <https://CRAN.R-project.org/package=geosphere>.

1189 105. Alexander DH, Novembre J, Lange K. Fast model-based estimation of ancestry in unrelated  
1190 individuals. *Genome Res*. 2009;19(9):1655-64. doi: 10.1101/gr.094052.109.

1191 106. Rosenberg NA. DISTRUCT: A program for the graphical display of population structure. *Mol Ecol  
1192 Notes*. 2004;4(1):2. doi: 10.1046/j.1471-8286.2003.00566.x.

1193 107. Jakobsson M, Rosenberg NA. CLUMPP: A cluster matching and permutation program for dealing  
1194 with label and switching and multimodality in analysis of population structure. *Bioinformatics*.  
1195 2007;23(14):6. doi: 10.1093/bioinformatics/btm233.

1196 108. Chen C, Durand E, Forbes F, François O. Bayesian clustering algorithms ascertaining spatial  
1197 population structure: A new computer program and a comparison study. *Mol Ecol Notes*.  
1198 2007;7(5):747-56. doi: 10.1111/j.1471-8286.2007.01769.x.

1199 109. Mitchell MW, Rowe B, Sesink Clee PR, Gonder MK. TESS Ad-Mixer: A novel program for  
1200 visualizing TESS Q matrices. *Conserv Genet Res*. 2013;5(4):1075-8. doi: 10.1007/s12686-013-  
1201 9987-4.

1202 110. Jombart T, Ahmed I. adegenet 1.3-1: new tools for the analysis of genome-wide SNP data.  
1203 *Bioinformatics*. 2011;27(21):3070-1. doi: 10.1093/bioinformatics/btr521.

1204 111. Anderson EC, Thompson EA. A model-based method for identifying species hybrids using  
1205 multilocus genetic data. *Genetics*. 2002;160(3):1217-29.

1206 112. Wringe BF, Stanley RRE, Jeffery NW, Anderson EC, Bradbury IR. hybriddetective: A workflow  
1207 and package to facilitate the detection of hybridization using genomic data in R. *Mol Ecol Res*.  
1208 2017;17(6):e275-e84. doi: doi:10.1111/1755-0998.12704.

1209 113. Wringe BF, Stanley RRE, Jeffery NW, Anderson EC, Bradbury IR. parallelnewhybrid: an R  
1210 package for the parallelization of hybrid detection using newhybrids. *Mol Ecol Res*.  
1211 2017;17(1):91-5. doi: doi:10.1111/1755-0998.12597.

1212 114. Gutenkunst RN, Hernandez RD, Williamson SH, Bustamante CD. Inferring the Joint Demographic  
1213 History of Multiple Populations from Multidimensional SNP Frequency Data. *PLoS Genet*.  
1214 2009;5(10):e1000695. doi: 10.1371/journal.pgen.1000695.

1215 115. Fitzpatrick MC, Keller SR. Ecological genomics meets community-level modelling of biodiversity:  
1216 mapping the genomic landscape of current and future environmental adaptation. *Ecol Lett*.  
1217 2015;18(1):1-16. doi: <https://doi.org/10.1111/ele.12376>.

1218 116. Láruson ÁJ, Fitzpatrick MC, Keller SR, Haller BC, Lotterhos KE. Seeing the forest for the trees:  
1219 Assessing genetic offset predictions from gradient forest. *Evol Appl*. 2022;15(3):403-16. doi:  
1220 10.1111/eva.13354.

1221 117. Frichot E, Schoville SD, Bouchard G, François O. Testing for associations between loci and  
1222 environmental gradients using latent factor mixed models. *Mol Bio Evol*. 2013;30(7):1687-99. doi:  
1223 10.1093/molbev/mst063.

1224 118. Turner SD. qqman: an R package for visualizing GWAS results using Q-Q and manhattan plots. *J  
1225 Open Source Software*. 2018;3(25):731. doi: <https://doi.org/10.21105/joss.00731>.

1226 119. Kinsella RJ, Kähäri A, Haider S, Zamora J, Proctor G, Spudich G, et al. Ensembl BioMarts: a hub  
1227 for data retrieval across taxonomic space. *Database*. 2011;2011:bar030. doi:  
1228 10.1093/database/bar030.

1229 120. Zerbino DR, Achuthan P, Akanni W, Amode M R, Barrell D, Bhai J, et al. Ensembl 2018. Nucleic  
1230 Acids Res. 2018;46(D1):D754-D61. doi: 10.1093/nar/gkx1098.

1231 121. Consortium GO. The Gene Ontology (GO) database and informatics resource. *Nucleic Acids  
1232 Research*. 2004;32(suppl\_1):D258-D61. doi: 10.1093/nar/gkh036.

## 1233 **Supporting Information**

1234 **S1 File. Supplemental Results.**

1235 **S2. File Extended Methods and Materials.**

1236 **S1 Fig. Origins of chimpanzees of Cameroon included in this study.** Sample

1237 locations and proportions of estimated ancestry were estimated in previous studies [83,  
1240 122].

1241 **Table S1. Captive chimpanzee genomes included in this study**

1242 **S2 Fig. Heterozygosity estimates of captive chimpanzee genomes.**

1243 (A) Individual heterozygosity.

1244 (B) Subspecies heterozygosity.

1245 **S3 Fig. Population structure of captive chimpanzee genomes.**

1246 (A) PCA of LD pruned SNP data set consisting of 1,113,142 SNPs.

1247 (B) sNMF individual ancestry analysis of the LD pruned data set in a range of K values.

1248 (C) PCA of Neutral SNP data set consisting of 147,000 SNPs.

1249 (D) sNMF individual ancestry analysis of the neutral SNP data set in a range of K  
1250 values.

1251 **S4 Fig. Cross Entropy Results.**

1252 Value of the cross-entropy criterion as a function of the number of ancestral populations  
1253 in sNMF for (A) the LD pruned SNP panel and (B) the neutral SNP panel.

1254

1255 **Table S2. Top 10 regions under selection including their genetic content.**

1256 **Table S3. Enriched GO terms in the “Biological Processes” domain.**

1257 **Table S4. Enriched KEGG pathways.**

1258 **Table S5. Functional enrichment clustering.**

1259 **Table S6. Number of wild chimpanzee samples collected and used in this study.**

1260 **Table S7. Environmental predictor variables used characterize chimpanzee  
1261 habitats.**

1262 **Table S8. Pearson correlation table of environmental variables.**

1263 **Table S9. Environmental variable groupings.**

1264 **S5 Fig. Illumina reads of wild chimpanzee samples evaluated into 4 categories.**

1265 Raw reads – yellow, mapped reads (sequence reads that mapped to the panTro4

1266 reference genome) – green, mapped and deduplicated reads (PCR duplicates were  
1267 removed) – light blue, and on-target reads mapped to our sites – dark blue.  
1268 (A) Proportion of read types for all 192 sequenced chimpanzee samples.  
1269 (B) Number of read types for 85 samples included in the '10k' dataset.  
1270 (C) Number of read types for samples removed due to missingness (>30% missing  
1271 sites).  
1272 (D) Proportion of read types for 85 samples included in the 'complete' dataset.  
1273 (E) Number of read types for duplicate samples removed following relatedness analysis.  
1274 (F) Number of read types for 23 individuals included in the '1k' dataset, but not the '10k'  
1275 dataset.

1276 **S6 Fig. Frequency of mean sequencing coverage of wild chimpanzee samples for**  
1277 **each site.**

1278 Mean coverage across all sites was 20.2 reads/site. The red vertical line represents the  
1279 minimum coverage needed to accurately call SNPs (5x coverage).

1280 **S7 Fig. Pairwise  $F_{ST}$  between sites shows population structure. (A) '10k' dataset.**  
1281 **(B) '1k' dataset.**

1282 **S8 Fig. Isolation-by-distance for '10k' dataset.**

1283 (A) Correlation between 'linearized  $F_{ST}$ ' and geographic distance (km) generated using  
1284 the '10k' dataset. Solid circles represent pairs of sampling locations from the same  
1285 habitat. Dual-colored diamonds represent pairs of sampling locations from different  
1286 habitats.

1287 (B) Null distribution of t-statistics from 10,000 permutations same- or different  
1288 habitat/population pairs in four bins of geographic distance. The red dotted line shows  
1289 the t-statistic value for actual data.

1290 **S9 Fig. Isolation-by-distance for '1k' dataset.**

1291 (A) Correlation between 'linearized  $F_{ST}$ ' and geographic distance (km) generated using  
1292 the '1k' dataset. Solid circles represent pairs of sampling locations from the same  
1293 habitat. Dual-colored diamonds represent pairs of sampling locations from different  
1294 habitats.

1295 (B) Null distribution of t-statistics from 10,000 permutations same- or different  
1296 habitat/population pairs in four bins of geographic distance. The red dotted line shows  
1297 the t-statistic value for actual data.

1298 **S10 Fig. Isolation-by-distance for only *P. t. elliotti* populations.**

1299 (A) Correlation between ‘linearized  $F_{ST}$ ’ and geographic distance (km) generated using  
1300 the ‘10k’ dataset. Solid circles represent pairs of sampling locations from the same  
1301 habitat. Dual-colored diamonds represent pairs of sampling locations from different  
1302 habitats.

1303 (B) Null distribution of  $t$ -statistics from 10,000 permutations same- or different  
1304 habitat/population pairs in four bins of geographic distance. The red dotted line shows  
1305 the  $t$ -statistic value for actual data.

1306 **S11 Fig. PCA of all SNPs from the ‘10k’ dataset.**

1307 The first two principal components recapitulate known population structure of  
1308 chimpanzees in Cameroon. They show 3 clear populations, and one *P. t. ellioti*  
1309 (Ecotone) individual (CMMD06) clustering with *P. t. troglodytes*, as well as multiple *P. t. t.*  
1310 *ellioti* (Rainforest) clustering together with *P. t. ellioti* (Ecotone) and vice versa.

1311 **S12 Fig. PCA of only neutral SNPs from the ‘10k’ dataset.**

1312 **S13 Fig. PCA of all SNPs from the ‘1k’ dataset**

1313 **S14 Fig. PCA of only neutral SNPs from the ‘1k’ dataset**

1314 **Table S10. The results of the Tracy-Widom test for all SNPs from the ‘10k’ SNP**  
1315 **dataset.**

1316 **S15 Fig. ADMIXTURE bar plots for  $K=2-3$ .**

1317 These three populations correspond to known population structure. However, at  $K=2$ ,  
1318 there is a signal of possible historic gene flow of *P. t. troglodytes* into *P. t. ellioti*  
1319 (Ecotone). Moreover, there is one individual (CMMD06 – also identified in the PCA) as  
1320 being a potential *ellioti/troglodytes* hybrid. At  $K=3$ , we see evidence of three additional  
1321 individuals that may be Rainforest/Ecotone hybrids, as well as evidence of mixing  
1322 between the populations.

1323 **S16 Fig. The cross-validation error results of ADMIXTURE analysis of wild**  
1324 **chimpanzees (‘10k’ dataset).**

1325 **S17 Fig. PCA results of the merged captive and wild datasets.**

1326 **S18 Fig. ADMIXTURE bar plots for  $K=2-5$  for merged captive and wild datasets.**

1327 **S19 Fig. The cross-validation error results of ADMIXTURE analysis of merged**  
1328 **captive and wild chimpanzees (‘10k’ dataset).**

1329 **S20 Fig. Cluster analysis and spatial interpolation of population structure.**

1330 (A) TESS bar plots showing individual proportions of ancestry of wild chimpanzees.

1331 (B) Spatial interpolation of the Q matrix for  $K=3$  generated using TESS and Ad-Mixer.

1332 **S21 Fig. Estimating  $K_{MAX}$  from TESS analysis.**

1333 DK values estimated for  $K=1-5$  across 10 replicate runs.

1334 **Table S11. Analysis of Molecular Variance (AMOVA).**

1335 **S22 Fig. Mean observed heterozygosity.**

1336 (A) Heterozygosity of all loci for all individuals grouped by population.

1337 (B) Heterozygosity for all individuals.

1338 There were no significant differences between heterozygosity for each population.

1339 **S23 Fig. Posterior plots of model performance.**

1340 (A) The observed Joint SFS for *P. t. troglodytes* and *P. t. ellioti*.

1341 (B) the simulated Joint SFS for *P. t. troglodytes* and *P. t. ellioti* under the most likely  
1342 asymmetric migration scenario obtained from  $\delta\alpha\delta\iota$ .

1343 (C) The residuals between the modeled and observed Joint SFS.

1344 (D) A 1D histogram of the residual values between the model and the observed data

1345 **S24 Fig.  $R^2$  weighted importance of the environmental predictor variables to the**  
1346 **Gradient Forest model of gene-environment relationships.**

1347 **S25 Fig. Results of randomized gradient forest models (n=200), as compared to**  
1348 **results from the observed data (n=200).**

1349 An average 588 of 7,878 SNPs demonstrated a positive  $R^2$  with at least one  
1350 environmental variable, with an average  $R^2 = 0.155$  in the Observed data distribution  
1351 (n=200, represented by the red histograms in A) and B) above). A significantly different  
1352 average was obtained when randomizing the associations between the genomic data  
1353 (SNPs) and environmental predictors for both total SNPs with a positive  $R^2$  (average  
1354 total = 504,  $t = 5.011$  (unequal variances  $df = 202.28$ ),  $p < 0.0001$ ), as well as for the  
1355 average  $R^2$  (average = 0.152,  $t = 2.806$  (unequal variance  $df = 261.97$ ),  $p = 0.0054$ ) of  
1356 the randomized gradient forests runs (n=200).

1357 **Table S12. Enriched GO terms in the ‘Biological Processes’ domain for**  
1358 **environmentally associated outliers (LFMM and gradient forest) in wild**  
1359 **chimpanzees.**

1360 **Table S13. Enriched KEGG pathways for environmentally associated outliers**  
1361 **(LFMM and gradient forest) in wild chimpanzees.**

1362 **Table S14. Enriched GO terms in the ‘Biological Processes’ domain for**  
1363 **environmentally associated outliers (LFMM and gradient forest) in wild**  
1364 **chimpanzees.**

1365 **S26 Fig. Evidence of selective pressures on acetyl-CoA acetyltransferase 2**  
1366 **(ACAT2).**

1367 (A) Map of the ACAT2 gene on chromosome 6 with brown star representing the SNP  
1368 identified through outlier analysis between *P. t. troglodytes* and *P. t. ellioti*.

1369 (B) Manhattan plot showing the significance (as the negative  $\log_{10}$  p-value) of SNP  
1370 associations with the environmental variable temperature seasonality. Grey colors  
1371 distinguish different chromosomes. The red line represents the threshold for significant  
1372 association ( $p = 0.05$ ). The SNP contained in the ACAT2 gene is highlighted by the red  
1373 arrow.

1374 (C) Correlation between the allele frequency of the SNP contained in the ACAT2 gene  
1375 and temperature seasonality values at each corresponding sampling location ( $R^2 =$   
1376 0.5615,  $p = 0.0005$ ).

1377 (D) Allele frequencies of the SNP contained in the ACAT2 gene across Cameroon.  
1378 Sampling sites are represented by circles that are shaded according to the frequency of  
1379 the allele within the population. SNP frequencies are plotted against temperature  
1380 seasonality across the region.

1381 **S27 Fig. Evidence of selective pressures on phospholipase C like 2 (PLCL2).**

1382 (A) Map of the *PLCL2* gene on chromosome 3 with brown star representing the SNP  
1383 identified through outlier analysis between *P. t. troglodytes* and *P. t. ellioti*.

1384 (B) Manhattan plot showing the significance (as the negative  $\log_{10}$  p-value) of SNP  
1385 associations with the environmental variable precipitation of wettest month. Grey colors  
1386 distinguish different chromosomes. The red line represents the threshold for significant  
1387 association ( $p = 0.05$ ). The SNP contained in the PLCL2 gene is highlighted by the red  
1388 arrow.

1389 (C) Correlation between the allele frequency of the SNP contained in the PLCL2 gene  
1390 and precipitation of wettest month values at each corresponding sampling location ( $R^2 =$   
1391 0.3422,  $p = 0.0102$ ).

1392 (D). Allele frequencies of the SNP contained in the PLCL2 gene across Cameroon.  
1393 Sampling sites are represented by circles that are shaded according to the frequency of  
1394 the allele within the population. SNP frequencies are plotted against precipitation of  
1395 wettest month across the region.